Distribution Agreement

In presenting this thesis as a partial fulfillment of the requirements for a degree from Emory University, I hereby grant to Emory University and its agents the non-exclusive license to archive, make accessible, and display my thesis in whole or in part in all forms of media, now or hereafter now, including display on the World Wide Web. I understand that I may select some access restrictions as part of the online submission of this thesis. I retain all ownership rights to the copyright of the thesis. I also retain the right to use in future works (such as articles or books) all or part of this thesis.

William T. Koval April 11th, 2017

The interactive effect of environmental stochasticity and resource driven intraspecific competition on *Culex quinquefasciatus* (Diptera: Culicidae) larval productivity

by

William T. Koval

Gonzalo M. Vazquez-Prokopec, MSc, PhD
Adviser

Department of Environmental Sciences

Gonzalo M. Vazquez Prokopec, MSc, PhD

Adviser

Uriel D. Kitron, MPH, PhD

Committee Member

Christopher W. Beck, PhD

Committee Member

2017

The interactive effect of environmental stochasticity and resource driven intraspecific competition on *Culex quinquefasciatus* (Diptera: Culicidae) larval productivity

By

William T. Koval

Gonzalo M. Vazquez-Prokopec, MSc, PhD

Adviser

An abstract of
a thesis submitted to the Faculty of Emory College of Arts and Sciences
of Emory University in partial fulfillment
of the requirements of the degree of
Bachelor of Sciences with Honors

Department of Environmental Sciences

2017

Abstract

The interactive effect of environmental stochasticity and resource driven intraspecific competition on *Culex quinquefasciatus* (Diptera: Culicidae) larval productivity
By William T. Koval

Members of the *Cx. pipiens* complex (*Cx. pipiens quinquefasciatus* in the Southern US) play a critical role in the spillover of urban arboviruses such as West Nile Virus or St. Louis Encephalitis virus. Field studies show strong correlation between the periodicity of rainfall events and larval proliferation in the vector's primary urban habitat: roadside catch basins. However, mechanistic determinants driving this relationship have not been empirically tested. I hypothesize that rainfall events decrease strain from exploitative intraspecific competition via the associated reduction of immature density and the introduction of detritus. To address my hypothesis, I used a deterministic matrix projection model consisting of an age-structured larval matrix coupled with a stage-structured adult mosquito matrix. Laboratory competition experiments were used to derive key model parameters, such as consumption, survivorship, and time to stage change. Consumption rate, calculated from mortality as a function of available resources, is an indirect measure used to inform the metabolic ages in the larval matrix. Generalized Linear Models of larval mortality from laboratory experiments were used as the metric for density-dependent population effects along a four-level nutrient gradient (0.375, 0.75, 1.5, 3 mg fish food per capita). Density-dependent effects were observed in the lower three treatment levels. The high density treatment (0.375 mg/larva) had the largest mortality rate at [0.0155 ± CI 0.0005 larvae/day, $p << 0.001$]. Despite variable time to pupation across treatments (17.07 ± CI 7.43 days), average day of metamorphosis in each treatment was associated with relatively consistent lifetime consumption (32.05 ± CI 0.07 mg/larva). Using experimentally informed metabolic ages, single and double rain event regimes were simulated and compared to a null model that did not account for competition. Variable rain delays in two-event simulations showed optimal proliferation occurring at a delay of 19 days between events. This is comparable to the pattern observed in natural populations, demonstrating that realistic *Cx. quinquefasciatus* proliferation rates can be modeled mechanistically as a density-dependent system. The empirical understanding of density-dependence as it relates to environmental stochasticity provides a theoretical platform for the study of larval dynamics and the impact of larval control in this medically relevant disease vector.

The interactive effect of environmental stochasticity and resource driven intraspecific competition on *Culex quinquefasciatus* (Diptera: Culicidae) larval productivity

By

William T. Koval

Gonzalo M. Vazquez-Prokopec, MSc, PhD

Adviser

A thesis submitted to the Faculty of Emory College of Arts and Sciences
of Emory University in partial fulfillment
of the requirements of the degree of
Bachelor of Sciences with Honors

Department of Environmental Studies

2017

Acknowledgements

I am grateful to Joseph R McMillan and Rebekah Blakney for their assistance in observation of in-lab larval competition experiments and for their patient, thoughtful advice in statistics, ecology, and scientific principles. Additionally, I would like to thank the Department of Environmental Sciences for helping to fund this project through the Lester Grant. Finally, many thanks Uriel Kitron, Christopher Beck, and Gonzalo Vazquez-Prokopec for their contributions to the intellectual work of this project through their role as committee members.

Table of Contents

Glossary of Terms

Abundance	Total number of individuals in a population
Arbovirus	Virus transmitted by an arthropod
Coeval	Individuals of the same age
Cohort	A coeval group of individuals
Competency	The ability of an individual to be a host
Consumption	The rate at which an individual or a population exploits the resources of an environment
Demography	The distribution of ages and characteristics across population
Deterministic Model	A predictive model whose outputs describe a relationship between input factors and which does not allow for random variability
Detritus	Organic material and litter entering an aquatic habitat
Emergence	Metamorphosis into Adulthood
Environmental Stochasticity	Random effects that affect all members of the population equally
Enzootic	Disease transmission cycle which is non-human in nature
Exploitation	Consumption of a resource by an individual which limits the intake of the same resource by others and ultimately reduces fitness of others
Extrinsic Factor	Factors that affect demography equally through environmental stochasticity
Fecundity	Maximum number of offspring able to be produced by a single female
Fertility	Number of realized offspring from single adult female
Gravid	Female mosquito that is ready to oviposit
Instars	The four larval stages of *Cx. spp.*
Intensity	The degree to which events occur, such as rainfall volume or total proliferation in a spike
Intrinsic Factor	Factors that affect demography disproportionately based on biological factors such as competition and consumption rate
Longevity	Lifespan of an individual or length of time that an insecticide remains in a habitat
Mesocosm	Experimental container large enough to support an immature population outside the lab and resemble a natural system
Metabolic age	Age of individual in terms of relative consumption rate of cohorts within the age distribution of a population where the oldest cohort enters pupation
Nutrients	The directly consumable metabolites for larval populations in a habitat produced via dissolution and bacterial decomposition
Periodicity	The length of time between two events, such as rainfall or proliferation spikes
Proliferation	Total number of individuals emerged (adult) or hatched (larvae) over a given time period
Proliferation Spike	The total number of individuals emerged (adult) or hatched (larvae) in synchrony. Used in reference to environmental periodicity
Reservoir Host	The long-term host of a pathogen
Spillover	The overflow of a transmission cycle into a dead-end host, generally humans, that will not support pathogen proliferation
Stable Age Distribution	The population state in which the absolute density of individuals changes but the proportion of age classes within the population is constant
Time age	Measure for age of individual in days
Urban System	The urban *Cx. quinquefasciatus* system is the standing water of roadside catch basins (Fig. 2) and the accompanying hypogenous drainage system. These habitats almost exclusively host *Cx. spp* and are of high organic content
Vector Host	An individual that acts as an agent to transmit a pathogen to another species

Introduction

First isolated in the West Nile of Uganda, West Nile Virus (WNV) has rapidly expanded across the globe [1]. WNV is a mosquito-borne flavivirus capable of infecting a variety of vector and reservoir host species [2]. The generalist nature of WNV lends to the observed range expansion along migratory bird corridors and across the wide geographic distribution of competent mosquito vectors [3, 4]. During initial geographic range expansion, WNV caused large epidemics in Romania, Russia, and Israel [2]. Thought to have traveled through Israel, WNV arrived in the U.S. via New York City in 1999 [5]. By 2002, WNV was observed across the eastern U.S. and within another two years had spread across the continent to become the most common arboviral disease within North America [3, 4]. The rise of WNV was associated with clinical cases ranging from mild fever to fatal neurodegenerative meningoencephalitis [3, 6]. By 2012, over 30,000 cases and more than 1,000 fatalities had been reported in the U.S. alone [4]. Case severity within the epidemic curves of WNV infection in human populations is influenced by both demography and spatial distribution [3]. Urbanization has been identified as a risk factor for overall WNV incidence in several studies [7-10]. This is likely due to the co-localization of the vector-reservoir transmission cycle (Fig. 1) and urban centers.

The transmission cycle of WNV is driven by mosquito vectors, which amplify transmission among avian reservoir hosts [4, 9, 11]. Members of the *Culex pipiens* complex have been identified as principal vectors for the viral transmission cycle due to their high abundance, competence, and infection rates observed in the field [4]. Individuals of this complex, *Cx. pipiens pipiens* in the northern U.S. and *Cx. pipiens quinquefasciatus* in the south, have been implicated in human WNV prevalence across the continent [4, 8, 12-15]. Culicine individuals have been shown to account for up to 96% of virus-positive pools while *Cx. pipiens* alone account for 88%

[4]. While many other species of *Cx. spp.* are enzootic and primarily ornithophilic, *Cx. quinquefasciatus* individuals have been shown to be opportunistic [4, 9, 16]. This combination of factors has led to the treatment of *Cx. quinquefasciatus* as the dominant vector of WNV, supported by epidemiological curve coincidence with *Cx. quinquefasciatus* proliferation [10, 15]. This is in contrast to other competent *Cx. spp.* vectors of WNV, which transmit WNV to avian reservoirs earlier in the season and outside the timing of peak human occurrence [9]. These early season rises in reservoir prevalence allow for later human spillover in urban centers by blooming *Cx. quinquefasciatus* populations [9, 17].

Due to this extensive role in human spillover cases, *Cx. pipiens* complex populations have been the subject of intense levels of vector control, primarily in urban areas. A variety of insecticides and biocides target different life stages of the vector, from larvae through pupae to adult. Adults have been shown to be knocked down by insecticide coils in lab, but these are not effective in the field due to resistance and low impact range [18-20]. However, the treatment of *Cx. quinquefasciatus* habitat in the urban core typically occurs through larvicidal application, proving to be expensive due to the large number of breeding sites [21-23]. Thus typical application is single to regular entry of toxin or growth suppressant into catch basins, the habitats of immature vectors [24]. The period of efficacy is dependent on duration of insecticide potency and environmental factors such as rain dilution effects and detrital loading within the catch basins [21, 24, 25]. High larvicidal efficacy (90-99% failed emergence) has been shown in lab-reared populations treated by Novaluron and *Bacillus thuringiensis israelensis* (BTI) [21, 26]. Nonetheless, realized efficacy against larval proliferation of the vector remains difficult to demonstrate in natural systems due to the high resistance of particular breeding sites to treatment [23]. This resistance stems from low mixing within larval populations and low efficacy of

larvicides in certain aquatic habitats due to interfering environmental factors. In addition, it has been demonstrated that *Cx. quinquefasciatus* individuals within urban systems were able to survive Novaluron treatment [21]. The longevity of these products is variable by design, but due to environmental constraints, can be as low as 7 days and as high as 105 days (Table 1) [21, 24].

Given the variable efficacy of larvicides, limited mosquito control budgets, public concerns about adulticides, and a lack of information on the spatial distribution of WNV transmission risk, most adult control is performed in response to the identification of infected mosquito pools or human cases. For instance, in Atlanta (GA) vector control is primarily performed using the larval control chemicals Altosid and Natular in response to WNV-positive mosquito pools in sentinel gravid traps to supplement limited regular control (Georgia Mosquito Control Association). Surprisingly, there is a lack of knowledge about the entomological and epidemiological impact of such interventions in the context of high environmental and climatic variability. This knowledge can best be obtained by first understanding *Cx. quinquefasciatus* natural history and physiology.

Cx. pipiens was first described in the *Systema Naturae* by Carolus Linnaeus in 1758 [27]. *Cx. quinquefasciatus* was originally distributed across the tropics of the New World and Southeast Asia [28, 29]. Described as an addition to the *Cx. pipiens* complex by Thomas Say in 1823, the vector was observed in great numbers along the Mississippi River basin [27]. Converse to many other vector mosquito species of African descent (e.g. *Aedes aegypti*, *Anopholes gambeii*), *Cx. quinquefasciatus* was likely introduced to Africa in boats returning from the Americas [30]. It is hypothesized that these long voyages selected for the ability to proliferate in confined habitat and an ability among the ornithophilic vectors to blood-feed on mammalian hosts [30]. These ships, whose bilges contained water highly contaminated with waste and

organic content, gave advantage to *Cx. pipiens* complex individuals over other genera due to the Culicine ability to thrive in such environments [30]. Indeed, the most common habitat of the species complex in urban areas of the U.S. is the catch basin drainage system, which possesses chemical properties similar to these bilges (Fig. 2) [24, 31]. In catch basins, *Cx. quinquefasciatus* individuals are released from the interspecific competition they experience in above-ground environments outside the urban system where they are only secondary vectors [4, 30].

Within both *Cx. quinquefasciatus* systems (epigeous rural and hypogeous urban), the relevance of the species as a disease vector has been noted through focused ecological study of their population dynamics. In the tropics of Hawaii, vector proliferation was seen to correlate with temperature and rainfall [32]. This same trend is observable within the urban catch basin system. For example, in Chicago, these two environmental factors were shown to explain up to 80% of WNV incidence [33]. While temperature rise is highly associated with WNV incidence and vector proliferation, rainfall effects have been shown to have more stochastic effects based on periodicity and intensity of events [15, 34]. Rainfall has a different role in urban areas due to the large accumulation of water and resources across the impervious drainage area for catch basins. It has been shown that there are both immediate and delayed responses to the temporal distribution of vector proliferation around rainfall events in urban systems [35].

Culicine eggs and pupae are easily flushed from flooded habitats [36]. Yet, at the temporally local scale, delayed increases in the rate of larval proliferation have been shown after flooding events [15, 33, 37]. This proliferation spike, occurring on average 4 days after a rain event, is associated with sharp declines in early instars and increases in female oviposition rates [37, 38]. Adult proliferation has also been demonstrated to be time-lag associated with rainfall events. Approximately two weeks are required for emergence spikes to occur and an optimal

periodicity of three weeks between rainfall events allows for oviposition and hatching to establish the next generation [33, 34]. Therefore, rainfall periodicity has an impact on vector proliferation comparable to the intensity of temperature change impact in the urban catch basin system at a finer temporal grain. Yet despite rainfall impact on temporally local vector proliferation, the intrinsic mechanisms driving this relationship are rarely empirically investigated in *Cx. quinqeufasciatus* and are sparingly considered within deterministic models [33-35, 38, 39].

In catch basin habitats, nutrient loading typically occurs through the introduction of detritus with rainfall, which can then be processed via dissolution and bacterial decomposition [40]. *Culex pipiens spp.* larvae use palatal brushes to filter planktonic bacteria and dissolved organics from the water column, as well as browsing decaying material adhered to surfaces [41]. Therefore, detritus has both an indirect and direct effect on larval mosquito resource availability. In systems of high detrital content, bacteria process organic substrates to maintain an equilibrium of internal nitrogen and carbon, which results in the excretion of produced metabolites [42]. The fluctuating metabolite concentrations have been shown to act as volatile kairomones that influence Culicine oviposition behavior [42-46]. It has been consistently demonstrated that oviposition preference for these high nutrient environments increases oviposition rates within catch basins [37, 47-50]. This preference contributes to the rarity of *Cx. pipiens* complex individuals in other aquatic environments, such as the limited-space, plastic containers preferred by *Aedes spp.* [30, 46, 51]. The *Cx. quinquefasciatus* strategy for oviposition selection is logical when realized with the fact that oviposition occurs through egg raft masses of approximately 200 coeval individuals [52]. The physiological nutrient requirements of the vector also complement this strategy. For example, the most attractant kairomones to ovipositing females are fatty acids

and esters, which are necessary for both egg production and flight muscle mechanics in emergent adult *Cx. quinquefasciatus* [46, 53].

Primarily, the physiological factors that distinguish the *Cx. pipiens* complex from other mosquito species are those that allow and require proliferation within high organic content aquatic habitats. *Cx. quinquefasciatus* individuals are one of the few insects confirmed in other studies, unique among other mosquitoes, which require more than 10 essential amino acids [54]. This implies a wider variety of nutrient resources required for proper *Cx. quinquefasciatus* development when compared to other species. They are further metabolically distinguished by feeble or absent salvage mechanisms to utilize deteriorated resources in purine and pyrimidine production, a common strategy among other dipterans [54]. This prevents *Cx. quinquefasciatus* from utilizing available, but low nutrient breeding sites that other mosquitoes, such as some *Aedes spp.*, inhabit [55, 56]. Though both of these factors result in habitat selection that releases the vector from interspecific competition, the high densities in which *Cx. quinquefasciatus* are found leaves the vector vulnerable to intraspecific competition through the exploitation of quality and essential nutrients.

In high density larval populations, the determining factors of intraspecific competition are per capita consumption and, consequently, population-level consumption [56]. Across taxa, it has been demonstrated that consumption rates increase with body size [57]. In species of granivorous beetles, it has been shown that body size exponentially increases with age [58]. In Culicine individuals, nutrient loading into enriched environments allows for basal consumption rates to be increased relative to low nutrient habitats [59]. In *Cx. quinquefasciatus*, mass accumulation through the conversion of resources into consumer biomass increases as a result of this consumption, along with higher fitness upon emergence [59]. It is assumed that *Cx.*

quinquefasciatus mass accumulation follows other insect models in that consumption rates continue to rise with biomass accumulation while efficiency of mass conversion decreases due to higher metabolic rates [58, 60]. Thus, the population-level consumption depends upon age structure of immatures and, if resources are limited, the population consumption rate will exponentially increase unless adjusted for by increased mortality.

Culicine individuals subjected to higher densities exhibit time delayed emergence, decreased fecundity, poor and uneven growth, and overall lower survivorship to compensate for population-level resource restrictions [37, 50, 59, 61-63]. However, density-dependent effects can become exacerbated at the smaller scales of larval populations and space availability typical of experimental studies [63]. When assumed to be applicable to natural systems, the results of these effects cause an immediate reduction in fertility through decreased survival rate of offspring to adulthood and a multiplicative, delayed reduction in generational output through decreased fecundity of their offspring upon emergence. Though various species of mosquitoes have been shown to produce growth retardants, these pheromones are not sufficient to alleviate density-dependent effects [62]. In order to maintain the high densities of larvae which urban catch basins hold, detrital loading must be substantial and frequent.

Study Hypothesis

The relationships established between rainfall events and vector proliferation, with subsequent spikes in WNV incidence, have not been analyzed from the perspective of the biology of the vector *Cx. quinquefasciatus*. The overarching research hypothesis of this study is that larval competition in the urban *Cx. quinquefasciatus* system is a large determinant of demographic responses to environmental stochasticity. In order to address this hypothesis, the

dynamics of *Cx. quinquefasciatus* were assessed in a series of experimental and theoretical activities (Fig. 3). The preliminary objective in this process was to empirically quantify the contribution of nutrient loading and population density to the larval dynamics of *Cx. quinquefasciatus*. The main objective was to utilize the data collected and found in literature to inform a deterministic mathematical model. This demographic model within a closed population was used to explore the interactive effects of rainfall, nutrient loading, and density on population-level dynamics within the urban *Cx. quinquefasciatus* system.

Methods

In-Lab Experiments

Following the methods described by Chaves et. al., I placed oviposition traps in the urban forest patch of Baker Woods on Emory University campus in Atlanta, GA [48]. These traps were black, plastic tubs of dimensions 34 x 45 x 12 cm and baited with a timothy hay-dog food infusion. Traps were left overnight in Baker Woods (Emory campus) in order to coincide with peak ovipositing activity of gravid females [49]. *Culex* mosquito egg raft masses were collected daily. A subset of 20 coeval egg rafts were imaged through a dissection microscope with a Leica camera and individual eggs were counted using ArcMap (Redlands, CA) software. Egg rafts were isolated in the wells of two 12 transwell plates into 5 mL of creek water each. Both plates, containing 10 egg rafts each, were incubated in a Caron Insect Growth chamber at 80% relative humidity and 20°C, which reflects the low range of conditions observed in the field (maximum annually ~25°C). The number of larvae hatched from each raft was recorded daily. After all larvae hatched, fertility was calculated by total hatched divided by total number of eggs. This process was repeated for a total of 40 egg rafts.

Egg rafts not used in fitness metric calculation were included in an assay to determine the influence of nutrient availability on immature life history traits (survivorship, time to stage change, and consumption rate). A four-level gradient of nutrient availability (see Table 2) was applied to microenvironments in Bioquip mosquito breeders (Fig. 4). Nutrients delivered were from a stock solution of 300 mg of baker's yeast and 300 mg fish food dissolved in 0.9 liters of creek water (Peavine Creek, a fairly unpolluted stream running close to Emory Campus) for a 1.5 mg/mL feed solution. Creek water was used to prevent larval exposure to fluoridated tap water.

Lower chambers of 20 mosquito breeders (five replicates by four treatments) were filled with 400 mL of creek water. The 400 mL was comprised of natural and stock-enhanced water to form the absolute nutrient gradient to which equal larval groups were subjected. The gradient used was determined by a 25°C pilot study that showed no density-dependent effects within the high nutrient treatment and significant mortality within the low treatment. To populate each microenvironment, 40 I instar larvae (10 from each of four egg rafts) were placed in each container ~24 hours after hatching. Containers were incubated at 20°C/80%RH. Mosquito development was monitored daily by counting and removing IV instar and pupal molts as metrics for time to pupation and emergence, respectively. Additionally, total number of larvae and pupae were counted to quantify daily mortality. This value was calculated for each microenvironment by subtracting the number of IV instar molts and number of live larvae from the number of live larvae on the previous day.

Semi-Natural Observational Study

Twelve navy, plastic bins 23 x 30 cm in surface area were perforated to drain at approximately 9 cm in depth with a drill bit 1.5 cm in diameter (Fig. 5). These bins were filled to maximum depth and subjected to the four-level starting nutrient concentration treatment outlined in Table 2 with three contemporaneous replicates per treatment. I placed these experimental mesocosms in Baker Woods for 40 days in a randomly determined 4 x 3 array. Four containers were randomly selected to house HOBO pendant temperature loggers to track water temperature and three HOBOs were placed around the site to track ambient air temperature. Every week, I monitored the biting adult population of the study area by establishing a transect of three light

traps around the experiment site. Light traps use heat (light bulb) and carbon dioxide (dry ice) as bait for female individuals searching for a blood-meal (Fig. 6).

Each day, I recorded the demography of *Culex spp.* individuals, including number of Culicine egg rafts, larvae, and pupae. Larval populations in each mesocosm were rounded to the nearest 25 individuals. In addition, *Aedes spp.* IV instar individuals were enumerated to account for interspecific effects not observed in the typical natural system of *Cx. quinquefasciatus*. Pupal molts of *Culex spp.* and *Aedes spp.* individuals were counted and removed. Detritus and abiotic conditions recorded daily include: water depth, plant-matter detritus (broad-leaved), and animal-matter detritus (drowned arthropods). Plant matter was measured as an estimate of surface area by percent of total bin surface area rounded to the nearest 5%. Animal matter, because it decays at a much faster rate than plant matter, was counted as a binary nominal measure of presence/absence [45].

Statistics

I analyzed the distribution of survivorship and time to emergence in larval competition experiments for normality by QQ-plots and determined the data were non-normal. Despite no transformation of the data, I used gaussian Generalized Linear Models (GLMs) to correlate larval death rates with time, where time was the independent variable and larval death rates were input as a continuous variable by day. GLMs were necessary in order to account for the non-normal data through an integrated link function that allows variance magnitude to be a function of predicted value. Produced for each nutrient treatment group, GLMs were used to predict survivorship over time across the density gradient. I did not account for random effects because there was high synchrony of development and mortality across replicates within each treatment.

The models were used as linear approximations for mortality because Kaplan-Meier plots of survivorship assume independence of right-censored data points [64]. In this case, right-censorship occurred through pupation and synchrony of larval cohort pupation prevented this from being a reliable assumption. All other life history traits of immature individuals were reported by simple mean and variance. These traits, specifically pupation rate and overall survivorship from larvae to pupae and pupae to adult, were compared via analysis of variance (ANOVA) means test. Results were further analyzed with Tukey Honestly Significant Difference (HSD) tests with an alpha of 0.05.

I compared semi-natural observation and model output through a two-sample Kolmogorov-Smirnov test with an alpha = 0.05. Information on the procedures for all statistical comparisons was derived from "A Primer of Ecology with R" by M. Henry H. Stevens (2009).

Model Development

I selected a matrix projection model to explore the role of larval competition in the urban *Cx. quinquefasciatus* system. The two factors contributing to the selection of a matrix model over other available options were the stage-based biology of *Cx. quinquefasciatus* and the need for understanding how these stages were differentially affected by extrinsic factors (Fig. 7). The matrix projection is a stage- or age-based population vector being multiplied iteratively by a transition matrix of associated survival and stage change probabilities [65, 66]. This simplification is not far removed from the biology of *Cx. quinquefasciatus* and has been utilized in the study of other insect populations [66, 67]. Adult and larval productivity within the urban system are easily determined from the model output, which is a daily population vector resulting

from each iteration of the multiplication cycle. I constructed two matrix projection models in order to investigate the hypothesis with these advantages in mind.

The first model (Model N*) constructed was a stage-based matrix projection following the work of Lefkovitch et. al. with the objective of providing a null model responsive to extrinsic environmental factors but ignorant of the intrinsic biological factors of *Cx. quinquefasciatus* [66]. The average time to pupation and emergence from across experimental treatments were used to calculate the daily proportion of stage changes. Life expectancy in adults was set to 22 days with a gonotrophic cycle of 7 days [52, 68]. Fertility (egg hatch rate) was determined by in-lab observation while fecundity of gravid females was assumed to be the average number of eggs per egg raft collected. The use of daily stage change rates allowed for each projection cycle (i.e. multiplication of the previous population vector by the deterministic transition matrix) to be the equivalent of a single day. A list of given days could be passed to the model in order to simulate a rain event along the projection cycle term. In Model N*, rain events only flushed eggs and pupae from the population vector, setting their survivorship equal to zero with no time delay in the effect [36]. I used the model runs to determine the temporally local effects of rain events on population dynamics. The two vital metrics of these dynamics were time to larval and adult proliferation spikes along with the intensity of those spikes. I analyzed these metrics in reference to the second model, designed to assess the density dependence hypothesis of the study.

The second matrix model (Model A) was designed to explore the hypothesis that density-dependent mechanisms drive population-level dynamics correlated temporally with rain events. These density-dependent interactions rely on the centrally assumed equation

$$S_{j.t} = {}^{\omega_t}/_{\Omega_j}$$

where the survivorship (S) of cohort j at time t is equal to the nutrients (ω) available at time t divided by a coefficient of competition (Ω) upon cohort j. The coefficient Ω is calculated by the summed exploitative limitations of all cohorts (1 through Z) on cohort j in the equation

$$\Omega_j = \sum_{1\rightarrow Z}^{i} C_i N_i \Big/ C_j$$

where the consumption rate (C) is treated as a proportional effect by each metabolic age 1 through Z on cohort j multiplied by the number of individuals in each cohort. Metabolic age in this instance refers to the relative consumption rate of each cohort. This calculation allows for the competition coefficient to equal the number of cohort equivalent individuals competing with j, favoring larger cohorts as is the case in natural systems [59].

For example, in a population of larvae, IV instar larvae may eat 10 times the amount of metabolites as I instar larvae. If 10 IV instar larvae and 100 I instar larvae cohabitate an environment, then Ω for the IV instar larvae can be calculated as 0.1 * 100 (for the effect of I instars) plus 1 * 10 (for the effect of fellow IV instars) for a total of 20 IV instar equivalents within the environment. In contrast, there are 200 I instar equivalents for the Ω value of the I instar cohort. In a coeval population, such as in the larval competition experiments, Ω is always equal to the number of individuals within the environment, and thus mortality due to competition effects can be used to calculate the consumption rate if ω is known. A description of all metrics used in calculation of model parameters can be found in Table 3.

The translation of lab data into model function is informed by GLMs of larval mortality (μ) from each nutrient treatment. I used mortality instead of absolute number of larvae to generate GLMs in order to eliminate the false inclusion of stage changes as density-dependent deaths. Taken as a proportion, the daily mortality curve of predicted dead individuals was subtracted from one and multiplied by 40 in order to calculate S of the coeval larvae in each microenvironment. The known level of metabolites added daily was divided by predicted survivorship to produce the final consumption rate function over time, assumed to be an exponential. The central assumption of this calculation is that density-dependent effects are occurring and that they do so with no time lag. This operation, shown below, was only performed over the lower three treatment groups through the time period for which competition associated deaths were observed.

$$S_{\omega}(t) = \left(1 - \mathrm{GLM}_{g}(\mu_{\omega} \sim t)\right) * 40$$

$$C_{\omega}(t) = {\omega(t)}\Big/{S_{\omega}(t)}$$

In order to more realistically represent the population consumption and the coefficient of competition within Model A, I expanded the consumer stage (larvae) into daily metabolic stages (Fig. 8). These stages were informed by the low nutrient treatment (t_0 = 0.375 mg/larva) consumption rate function, where matrix time age was associated with the corresponding consumption rate of each metabolic age 1 through Z calculated experimentally.

The intercepts of all calculated consumption rate curves were correlated with starting per capita resources for respective experimental larval groups. The resulting correlation allowed for

newly hatched cohorts to be placed at a metabolic age (d) along the low nutrient consumption function to generate maximum exploitation of resources for I instar larvae at a given density. This calculation was capped at the intercept of the high nutrient consumption rate on the low nutrient consumption function trend (d_f). This was the case because no density-dependent effects were observed in this treatment and stage change was synchronized to indicate maximum rate of mass accumulation. Metabolic age Z, here 43 days, was determined from the appropriate time to pupation from d_f.

Within the larval transition matrix of Model A, survivorship was determined daily based on the tracked resources for larvae. This value for each cohort allowed movement to the next metabolic stage until age Z when larvae where permitted to pupate. This corresponds to the observed dynamics in experimentation that show delayed growth to pupation in lower nutrient environments. The other three stages from Model N* (Eggs, Pupae, and Adults) maintained structure in Model A because I assumed that no intrinsic effects occur at these stages within catch basins. I termed the model, structured as a combination of an explicit larval transition matrix of metabolic ages and daily-adjusted single probability change of other stages, a focal-stage matrix. Similar adjustment within matrix projection models has been done in parous cycles of tsetse flies [67]. However, this method is novel in the *Cx. quinquefasciatus* system . Ahumada et. al. utilized a similar method to analyze *Cx. quinquefasciatus* along temperature gradients, but this was performed across all immature stages in response to environmental stochasticity and did not have a dynamic survivorship parameter [32].

After determining the transition matrix of Model A, I simulated the projection cycle with zero, one, or two rain events of equal size. At each rain event, all pupae and eggs were flushed from the system as in Model N*. Additionally, 1 kg of detritus was introduced to each of 40

simulated catch basins for a total of 40 kg introduced into the system. The catch basin count is approximately the size of past study sites in the Atlanta area. I assumed that the accretion of litter and detritus will occur on average from a 10 m^2 drainage area per catch basin with 100 g / m^2 across that drainage area. The decay rate was set to 0.1% of matter being converted into directly consumable resources for larvae each day through bacterial decomposition. Populations in single rain event systems were observed for timing to first peak of adults while double event simulations were observed for optimal delay between rain events for proliferation.

Model Analysis

I compared Models N* and A visually through LOESS regression in response to a series of two-rain event simulations with variable periodicity. The comparison was made based on absolute proliferation of adults, average stage of population, and whether the population reached a stable age distribution. This comparison isolates the effects of density dependence as the determining model mechanism in response to rainfall events of equal intensity.

Additionally, I performed a sensitivity analysis on Model A to investigate the effect of $\omega(t)$ within consumption rate calculation and the effect of altered consumption rate on larval dynamics. The function for resource loading during experimentation was adjusted to either [1.33 * $\omega(0)$], Model B, or [0.66 * $\omega(0)$], Model C to simulate an increase or reduction in consumption, respectively. I made the same comparisons between Models A, B, and C that were used to compare Models N* and A. For each of these models, a LOESS regression of larval proliferation spikes was used to calculate the carrying capacity of the system (K). Carrying capacity was calculated through simple LOESS regression of model output for larval proliferation in Models A, B, and C. Time to extinction was calculated by extending the reduction of K at time 0 and time 100 to set K equal to zero.

Finally, data from the semi-natural observational study was compared to model output based on initial conditions and observed adult population. This was done using a two-sample Kolmogorov-Smirnov test despite the known sensitivity of the test to small sample size.

Assumptions

Model A assumes an absolute exploitative competition response within the larval population. This means that each day, larvae will consume the amount of nutrients designated by their metabolic age that are available to them. If this immediate need cannot be met, the model then assumes that mortality due to lack of nutrition operates on a zero time-lag response interval. This results in rapid mortality of cohorts if nutrients are exhausted from the environment.

Relating to the simulated urban system, the model assumes consistent distribution of detritus temporally so that rain events close together in time will have the same amount of nutrient loading into catch basins. Additionally, it assumes that the effects of evaporation within the system are negligible. Finally, oviposition site selection of *Cx. quinquefasciatus* females within the model is strictly adherent to catch basin habitats. This prevents mixing of epigeous and hypogeous populations and creates a closed population across the number of simulated catch basins.

In reference to the biology of *Cx. quinquefasciatus*, the model assumes a low efficiency of resource processing and mass accumulation, particularly in low nutrient environments. This is compounded by the assumption that larvae do not eat the processed waste of other larvae and do not consume the bodies of larvae who have died as a consequence of density dependence. This up-regulates the rate at which nutrients leave the system within Model A.

Results

In-Lab Experiments

Egg rafts collected from the field for fertility analysis and later identified as *Cx. quinquefasciatus* (n = 29) contained on average 258 ± 23.0 eggs (± 95% CI). The hatch rate of these egg raft masses was on average 91.0 ± 6.5% of individuals. Time to hatching was highly synchronized within egg rafts, occurring simultaneously 2-3 days after oviposition. Because 82.8% of rafts hatched on day 2 rather than day 3, I assumed the rate of stage change from egg to larvae when applied in Models N* and A to be 2 days.

Life history trait parameters (survivorship, rate of stage change) of larval competition experiments are listed in Table 4. I did not calculate emergence rate by pupae because individuals were not tracked from time to pupation through emergence. Instead I used total time to emergence (Fig. 9). However, the difference between mean time to pupation and mean time to emergence for all individuals within the experiments could be observed and was fairly constant with a mean of 2.8 days (Fig. 9). Additionally, pupal survivorship to adulthood was consistent, ranging from a calculated value of 93.0% to 99.0% ($F = 0.5; p = 0.73$) (Table 4, Fig. 10). Survivorship from the larval stage to pupation decreased along the nutrient gradient (Fig. 10) from 99 ± 1.0 survivorship in the highest nutrient environment to 23.5 ± 11.6% in the lowest treatment (Table 4). Larval survivorship varied across nutrient treatment with the two lower nutrient treatments were significantly different from the two higher treatments and each other ($F = 102.6$; $p << 0.001$) (Fig. 10). Thus, strength of competitive effects was inversely correlated with nutrient availability.

Mortality curves produced using GLMs for each nutrient treatment (Fig. 11) showed significant associations between time and larval deaths in treatments where density-dependent

effects were observed (Low through Mid-High). Despite the sigmoidal nature of observed larval mortality (Fig. 11), GLMs were calculated as a linear relationship between deaths and time of the form

$$\mu_{\omega}(t) = \mathrm{N} * t + \mathrm{intercept}$$

The parameters of these curves are shown in Table 5. The steepest GLM slope, as would be assumed by the survivorship data in Table 4, belonged to the mortality curve of the low nutrient treatment, which was predicted to lose an average of 3 larvae every two days. Upon exponentiation of these three mortality curves through the consumption rate function calculation method, increase in consumption approached a linear relationship as nutrient availability increased (Fig. 12). Additionally, the basal consumption rate of I instar larvae (i.e., the intercept of the consumption function) increased with starting per capita nutrients from 0.4 mg to 1.8 mg of daily consumption per I instar larva (Fig. 12). When the per capita consumption rate functions were totaled cumulatively over the duration of the experimental trial (Fig. 13), pupation, though temporally variable (Table 4), was associated with a consistent predicted lifetime consumption of 32.05 ± 0.07 mg per larva.

Model Application

The parameters incorporated into Model N* and Model A are shown as transition matrices in Table 6 (schematic, Fig. 4). Apart from the larval matrix in Model A, the two transition matrices are identical. In Model A, single rain events (RE) at the start of new simulated seasons achieved larval and adult proliferation spikes at day RE + 5 and day RE + 14, respectively. A sample model simulation with a starting adult population of 200 adults within the described simulation system is shown in Figure 14. The model allows for both males and

females in the larval stage due to their equal contribution to competition effects. Both models remove males through the adult sub-matrix, discounting the mating process through a random mixing assumption and still including larval males in intraspecific competition. An initial population of 200 adults was selected for the simulation based on typical resting behavior of *Culex quinquefasciatus* individuals, assuming here 5 adults per catch basin on average.

In this example, boom and bust dynamics are easily observed, being more volatile within immature populations (Fig. 14). After resources have been diminished through direct decomposition and subsequent consumption by immature individuals, peaks of adult proliferation continue to occur with more controlled larval oscillations. This region of model output (i.e. beyond the first two proliferation cycles) is considered stable due to these reduced oscillations. The stable region is well-suited for testing model response to secondary input, so a second rain event was simulated to investigate the effects of rain on the age structure of a simulated population (Fig. 15). In a small larval population of the model, such as that of the pre-rain stable period, the age distribution is driven towards larger instars that can easily pupate. However, the introduction of detritus allows for the survival of otherwise threatened I instar larvae and disperses the otherwise stable immature metabolic age distribution.

In paired rain event simulations, the proliferation rates of Models N* and A were quantified by adult proliferation after 50 days from an initial population of 200. Rain events were simulated at RE = 2 and RE = 2 + t, where t was a delay ranging from 1 to 49 days, and then taken as a ratio to single rain event simulations with RE = 2 (Fig. 16). A 50 day monitoring period was selected in order to capture the first peak and decline of adult proliferation seen within the Model A single-event simulation. The LOESS regression associated with Model N* accelerated exponentially towards baseline after rainfall periodicity was greater than 40 days.

However, adding realism, as in Model A, altered the proliferation rate to produce regression to a peak value at 19 days, which is consistent with observed mosquito growth trends in urban environments [33, 34]. To more clearly understand the implications of the rain delay simulations, the model output of proliferations was condensed to boxplots (Fig. 17). In these plots, which denote the range of proliferation values relative to baseline growth of a single rain event for the rain delay period of day one through seven within each week, it can be seen that the most reliable increase in proliferation occurs over the range of week three (days 15 - 21).

Model Sensitivity

I subjected Model A to sensitivity analysis by altering the initial $\omega(t)$ function used to calculate consumption rate for the larval sub-matrix. This basal value change resulted in Model B, with increased ($1.33 * C_A$) consumption, and Model C, with decreased ($0.66 * C_A$) consumption. Total proliferation (adults emerged and eggs oviposited), efficiency of proliferation (mass of nutrients consumed per adult emerged), and population time to extinction were altered as a result (Table 8). Proliferation efficiency was an outlier among proportional responses by Models B and C as fractions of Model A. While Model A immature populations consumed 420 mg per Adult produced, Model B populations consumed 410 mg/adult and Model C consumed 480 mg/adult (Table 8). This implies an inverse relationship between per capita consumption and population consumption within model generations, which can be noted through the lowered yield of adults per egg raft (Table 8). As more individuals enter a low consumption system, they can overload carrying capacity more quickly and lead to more volatile boom-bust cycles.

These dramatic boom-bust cycles are apparent in the proliferation trends of Model C (Fig. 18). High intensity larval proliferation spikes continue to follow a single rain event due to lower per capita nutrient requirements. Model B behaved more similarly to Model A, with a rapid tapering into a stable dynamic. To investigate this comparison further, the same paired-event simulation test used to compare Models N* and A was run on Models B and C (Fig. 19). Model C followed a similar pattern to Model A, with regression towards an optimum periodicity for proliferation. However, the timing of this peak in proliferation differs from the literature. Model B appeared to be under high population pressure from increased consumption, and therefore responded positively to rain events on a shorter time delay than both Models A and C.

Semi-Natural Observation

Aggregate larval populations across semi-natural mesocosms as well as divisions by treatment are shown in Figure 20. Oviposition preference of higher nutrient habitats immediately presented an equalizing force in per capita nutrient distribution across mesocosms. This led to all environments behaving similarly in terms of observed mortality due to competition. The adult population of the study area was split mostly between Culicine species and *Aedes albopictus* (Table 7). Of the 156 adult females collected, 84 were *Culex spp.* and of these 43 were identified as *Cx. quinquefasciatus*.

Compared to Model A, observed data trends were significantly different according to a Kolmogorov-Smirnov test statistic of $D = 0.69$; $p << 0.001$ for larval population comparison and $D = 0.45$; $p = 0.006$ for the egg population. Though the intensity of both observed and simulated values are similar, the shape of the mortality curves are not. This effect is amplified when considering that although ~69 *Cx. spp* individuals emerged in observed data, no larvae reached

the pupal stage in the model run. Complications due to *Aedes spp.* presence make the estimate of observed Culicine pupae approximate.

Due to this discrepancy, a I compared the behavior of a Model A stable region peak with the behavior of the aggregate of observed values in semi-natural mesocosms (Fig. 21A). In both cases, observed and simulated, a select group of larvae pupate early on while others are left in an environment that exhibits the marks of density-dependent competition (high mortality, no population growth). As in the case of the mortality curves of in-lab larval competition, the mesocosm experiment demonstrates a sinusoidal decline after reaching peak larval proliferation. This demonstrates a consistency between the tendencies of natural systems in *Cx. quinquefasciatus* and Model A predictions. However, when model time is scaled to the semi-natural experiment duration (32 days), it is evident that the speed with which these patterns occur differs between simulation and reality (Fig. 21B). This could be due to a reduction in oviposition preference for the mesocosms by gravid *Cx. quinquefasciatus*. Oviposition declined from 20 rafts/day to less than 5 rafts/day by the end of the first 4 days of the observation period.

Discussion

The purpose of this study was to develop experimental data and a novel modeling technique to characterize the mechanisms driving the established pattern correlating *Cx. quinquefasciatus* proliferation with rainfall events. In the exploration of this purpose, several key ideas were put forward, namely on mortality, periodicity, and efficiency of the *Cx. quinquefasciatus* urban system.

The in-lab experiments done in this study confirm previous work done with *Cx. quinquefasciatus* [41, 54, 61, 69]. Pupae of larval experimental groups were shown to only be affected by larval survivorship. This suggests that time to pupation is strictly determined by mass accumulation and that emergence is a constant life stage change which is derived from consistent resource reserve processing. Despite reported variability in size upon emergence, it seems that the timing of resource reserve conversion into emergence potential is constant. This implies that pupation operates independent of absolute size, unlike larval survivorship and pupation. As mentioned, these experimental studies can bias the importance of density-dependence effects for mosquito biology, so it was necessary to realize the predicted population responses of *Cx. quinquefasciatus* with observations of larger scale [63]. Without confirmation of model trends at larger, more realistic scales of *Cx. quinquefasciatus* abundance, the significance of the model cannot be understood.

For this purpose, I conducted a semi-natural study and compared general shape of population response to resource reduction to that of a simulated population (Fig 21A). From this comparison, I saw a similarity between the number of larvae and pupae produced from habitats of limited resources. The semi-natural study demonstrated that density-dependent effects can occur in natural populations similar to the observed abundance in catch basin. Without the

nutrients necessary to fuel the boom of oviposition into semi-natural mesocosms, few individuals pupated and larvae began to be replaced by *Aedes spp.* (data not shown). This may suggest that it is pollutant tolerance, not nutrient acquisition as has been suggested, that allows for *Cx. quinquefasciatus* dominance in urban areas [7, 31]. In addition to these theoretical proposals, the semi-natural observation confirmed results of previous oviposition studies [37, 48].

The empirical data gathered through experiments were used to assess the realism of the biological and ecological assumptions imposed on the models. Primarily, mortality due to competition was highly synchronized in both mesocosm and in-lab experiments. This supports the model assumption that a zero time-lag survivorship response is reasonable at multiple scales. This assumption is most problematic when considering the initial boom and bust dynamics of novel immature habitats (Figs. 14 & 21). These large proliferation spikes are sharply adjusted by mortality rates that reflect the slope of sinusoidal trends observed in the data but on a maladjusted time scale. This stems from the calculation assumption that linear GLMs of mortality are adequate to capture and subsequently represent the density-dependent effects on survivorship and time to emergence. While this time-lag assumption poses little issue at larger scales (Fig. 16), it prevents adequate representation of trends from initial conditions. Nonetheless, I propose that these assumptions are supported by the shape of larval proliferation curves in both observed and published data (Figs. 16 & 21A).

To empirically quantify the contribution of nutrient loading and consumption to proliferation of *Cx. quinquefasciatus*, I performed a sensitivity analysis of Model A (Table 8). The most apparent result of analysis was the low sesntivity of larval proliferation in response to increased consumption rate in Model B while a disproportionate rise in other metrics was seen from Model C. This could be due to a lower bound of larval competition assumed by the model.

The production efficiency and time to extinction resulting from carrying capacity extrapolation were the more informative metrics to arise from this analysis. Efficiency of resources (both nutrients and progeny) varied disproportionately to the adjusted consumption rate parameters. Nutrient conversion to mosquito biomass was less efficient in low consumption populations, presumably due to the high rate of able colonization by ambient gravid females. A weighted age distribution towards lower consumers in this population (Model C) created a simulation that allowed for explosive growth beyond carrying capacity, resulting in higher mortality than the more conservative Model B. The surprising result from this analysis was the high yield of adults per raft in Model B (18-19 emergences per raft of 260 individuals) and the more efficient conversion of resources despite higher per capita consumption requirements. I propose that consumption limitations drove age structure in favor of higher instar individuals that were able to outcompete new hatchling I instars. This is complemented by the age structure plots derived from Model A (Fig. 15), which demonstrated age variance expansion in response to nutrient loading. New, I instar cohorts that are released from competition upon hatching in these conditions could be driving the spiked proliferation patterns observed in nature.

The pattern of population cycling would arise due to the model assumption that *Cx. quinquefasciatus* are highly exploitative and inefficient consumers, converting little nutrient into biomass. Indeed, this was observed through the high nutrient requirements predicted to produce a single adult (420 mg / 2 mg adult; Model A, Table 8). Nutrients leaving the model system through larval acquisition and mortality can help to explain the extensive role of this assumption. Given the extensive literature on the high nutrient requirements of *Cx. quinquefasciatus*, this assumption could hold if the advantage given to Culicine individuals is tolerance of catch basin pollution instead of resource acquisition within such environments [30, 41, 48, 50, 53, 54, 69].

Secondarily, time to extinction taken as a decrease in carrying capacity (K) to zero led to interesting notes on the model. The length of time to extinction (from 1300 to 2500 days; Table 8) is highly unrealistic not only due to seasonality, but to evaporation as well. I ignored these two critical factors in annual *Cx. quinquefasciatus* production because the goal of this study was to examine temporally local effects by the periodicity of stochastic events. Despite this stray from reality, time to extinction can still inform the study on how resources are exiting the system. In the case of Model A, a stable region lasts for such a duration (2500 hypothetical days) because of efficient proliferation in addition to high numbers of adults emerging. Both Models B and C have one of these characteristics (efficiency and abundance, respectively), but the combination of a stable adult population and high mass retention allows for continuous proliferation in Model A. If the model theory is to be applied to the urban catch basin system, these two factors associated with high nutrient loading could be the key to successful colonization and productivity in nature.

Conclusions

Replication of natural behavior within the *Cx. quinquefasciatus* system can be achieved through modeling immature populations as density-dependent. Model behavior was consistent with patterns shown at the broad urban scale present in literature and the fine-scale mesocosm experimentation conducted in the study. When competition was removed from this model, initial populations relied on, but then were suppressed by, rain events regardless of periodicity. At temporally local scales, the experimentally and theoretically described density-dependent mechanisms can regulate proliferation spikes. With the assumptions of this study in mind, it appears that hot-spot characteristics of proliferation can be modeled as reliant on the boom and bust dynamics inherent in the high nutrient, but high competition, *Cx. quiquefasciatus* habitat.

Driven by nutrient loading through stochastic rain events, these density-dependent interactions may have been overlooked due to the seasonal nature of WNV and *Cx. quinquefasciatus* surveillance. However, investigation into the mechanistic forces behind demographic response to environmental factors can be used to more thoroughly understand the proliferation blooms that are the target of vector management.

Future Directions

A secondary objective in the design of this project was to utilize modeled mechanistic behavior to inform vector management practices. Knowledge of age distribution dynamics within a system and how that system responds to nutrient loading is critical for understanding response to disturbance regimes such as insecticide application. This is particularly true of systems without guaranteed efficacy, and in fact almost guaranteed failure in some cases, of such regimes [23, 24]. Preliminary work within this model has shown that larvicidal application can alter the stage structure of an immature population (Fig. 22). Using data from Table 1, larvicides were simulated to kill 90% of IV instar larvae (as Natular would) for 35 days during the stable region of Model A (Fig. 23) [22, 70]. A rain event was either simulated at the end of this period or the insecticide was deemed inefficacious after 5 weeks. The exploratory results show that population recovery through age synchrony is possible and can surpass baseline proliferation in situations where per capita resources are increased through population reduction and rainfall occurrence (Fig. 23). This raises questions on the interaction between competition release and insecticide regime efficacy. The interplay between these two factors, though little studied, can aid in many vector management systems [10, 23, 24, 70, 71]. To expand upon the current study, an

investigation theoretically within the model and experimentally in the field would elucidate the answers to these questions.

References

1. Kramer, L.D., J. Li, and P.Y. Shi, *West Nile virus.* Lancet Neurol, 2007. **6**(2): p. 171-81.
2. Campbell, G.L., et al., *West Nile virus.* Lancet Infect Dis, 2002. **2**(9): p. 519-29.
3. Grubaugh, N.D. and G.D. Ebel, *Dynamics of West Nile virus evolution in mosquito vectors.* Current Opinion in Virology, 2016. **21**: p. 132-138.
4. Andreadis, T.G., *The Contribution of Culex pipiens Complex Mosquitoes to Transmission and Persistence of West Nile Virus in North America.* Journal of the American Mosquito Control Association, 2012. **28**(4s): p. 137-151.
5. Sambri, V., et al., *West Nile virus in Europe: emergence, epidemiology, diagnosis, treatment, and prevention.* Clinical Microbiology and Infection, 2013. **19**(8): p. 699-704.
6. Garcia, M.N., R. Hasbun, and K.O. Murray, *Persistence of West Nile virus.* Microbes and Infection, 2015. **17**(2): p. 163-168.
7. Brown, H.E., et al., *Ecological factors associated with West Nile virus transmission, northeastern United States.* Emerg Infect Dis, 2008. **14**(10): p. 1539-45.
8. Savage, H.M., et al., *Host choice and West Nile virus infection rates in blood-fed mosquitoes, including members of the Culex pipiens complex, from Memphis and Shelby County, Tennessee, 2002-2003.* Vector Borne Zoonotic Dis, 2007. **7**(3): p. 365-86.
9. Molaei, G., S. Huang, and T.G. Andreadis, *Vector-Host Interactions of Culex pipiens Complex in Northeastern and Southwestern USA.* Journal of the American Mosquito Control Association, 2012. **28**(4s): p. 127-136.
10. Andreadis, T.G., et al., *Epidemiology of West Nile Virus in Connecticut: A Five-Year Analysis of Mosquito Data 1999b.* Vector-Borne and Zoonotic Diseases, 2004. **4**(4): p. 360-378.
11. Diuk-Wasser, M.A., et al., *Avian communal roosts as amplification foci for West Nile virus in urban areas in northeastern United States.* Am J Trop Med Hyg, 2010. **82**(2): p. 337-43.
12. Kilpatrick, A.M., et al., *West Nile virus risk assessment and the bridge vector paradigm.* Emerg Infect Dis, 2005. **11**(3): p. 425-9.
13. Molaei, G., et al., *Vector-host interactions governing epidemiology of West Nile virus in Southern California.* Am J Trop Med Hyg, 2010. **83**(6): p. 1269-82.
14. Liu, H., Q. Weng, and D. Gaines, *Geographic incidence of human West Nile virus in northern Virginia, USA, in relation to incidence in birds and variations in urban environment.* Science of The Total Environment, 2011. **409**(20): p. 4235-4241.
15. Vazquez-Prokopec, G.M., et al., *The risk of West Nile Virus infection is associated with combined sewer overflow streams in urban Atlanta, Georgia, USA.* Environ Health Perspect, 2010. **118**(10): p. 1382-8.
16. Hamer, G.L., et al., *Culex pipiens (Diptera: Culicidae): a bridge vector of West Nile virus to humans.* J Med Entomol, 2008. **45**(1): p. 125-8.
17. Hongoh, V., et al., *Expanding geographical distribution of the mosquito, Culex pipiens, in Canada under climate change.* Applied Geography, 2012. **33**: p. 53-62.
18. Paul, A., et al., *Insecticide resistance in Culex pipiens from New York.* J Am Mosq Control Assoc, 2005. **21**(3): p. 305-9.
19. McAbee, R.D., et al., *Pyrethroid tolerance in Culex pipiens pipiens var molestus from Marin County, California.* Pest Manag Sci, 2004. **60**(4): p. 359-68.
20. Xue, R.-D., et al., *Insecticidal Activity of Five Commercial Mosquito Coils Against Anopheles albimanus, Aedes albopictus, and Culex quinquefasciatus.* Journal of the American Mosquito Control Association, 2012. **28**(2): p. 131-133.
21. Su, T., et al., *Laboratory and Field Evaluations of MosquironB. 0.12CRD, a New Formulation of Novaluron, Against Culex Mosquitoes.* Journal of the American Mosquito Control Association, 2014. **30**(4): p. 284-290.

22. Harbison, J.E., et al., *Evaluation of Culex pipiens Populations in a Residential Area with a High Density of Catch Basins in a Suburb of Chicago, Illinois.* J Am Mosq Control Assoc, 2014. **30**(3): p. 228-30.
23. Harbison, J.E., et al., *Identification of Larvicide-Resistant Catch Basins from Three Years of Larvicide Trials in a Suburb of Chicago, IL.* Environmental Health Insights, 2014. **8**(S2).
24. Harbison, J.E., et al., *Variable Efficacy of Extended-release Mosquito Larvicides Observed in Catch Basins in the Northeast Chicago Metropolitan Area.* 2016.
25. Harbison, J.E., et al., *Evaluation of Culex pipiens Populations in a Residential Area with a High Density of Catch Basins in a Suburb of Chicago, Illinois.* Journal of the American Mosquito Control Association, 2014. **30**(3): p. 228-230.
26. Cetin, H., et al., *Operational Evaluation Of VectomaxB. WSP (Bacillus thuringiensis Subsp. israelensis + Bacillus sphaericus) Against Larval Culex pipiens in Septic Tanks.* Journal of the American Mosquito Control Association, 2015. **31**(2): p. 193-195.
27. Harbach, R., *Culex pipiens: Species Versus Species Complex b.* Journal of the American Mosquito Control Association, 2012. **28**(4s): p. 10-23.
28. Linthicum, K.J., *Summary of the Symposium Global Perspective on the Culex pipiens Complex in the 21st Century: The Interrelationship of Culex pipiens, quinquefasciatus, molestus and Others.* Journal of the American Mosquito Control Association, 2012. **28**(4s): p. 152-155.
29. Turell, M.J., *Members of the Culex pipiens Complex as Vectors of Viruses.* Journal of the American Mosquito Control Association, 2012. **28**(4s): p. 123-126.
30. Farajollahi, A., et al., *"Bird biting" mosquitoes and human disease: a review of the role of Culex pipiens complex mosquitoes in epidemiology.* Infect Genet Evol, 2011. **11**(7): p. 1577-85.
31. Munstermann, L.E. and G.B. Craig, *Culex Mosquito Populations in the Catch Basins of Northern St. Joseph County, Indiana.* Proc Indiana Academy of Science, 1977(86): p. 246-252.
32. Ahumada, J.A., D. Lapointe, and M.D. Samuel, *Modeling the population dynamics of Culex quinquefasciatus (Diptera: Culicidae), along an elevational gradient in Hawaii.* J Med Entomol, 2004. **41**(6): p. 1157-70.
33. Ruiz, M.O., et al., *Local impact of temperature and precipitation on West Nile virus infection in Culex species mosquitoes in northeast Illinois, USA.* Parasit Vectors, 2010. **3**(1): p. 19.
34. Shand, L., et al., *Predicting West Nile Virus Infection Risk From the Synergistic Effects of Rainfall and Temperature.* J Med Entomol, 2016.
35. Lebl, K., K. Brugger, and F. Rubel, *Predicting Culex pipiens/restuans population dynamics by interval lagged weather data.* Parasit Vectors, 2013. **6**: p. 129.
36. Koenraadt, C.J. and L.C. Harrington, *Flushing effect of rain on container-inhabiting mosquitoes Aedes aegypti and Culex pipiens (Diptera: Culicidae).* J Med Entomol, 2008. **45**(1): p. 28-35.
37. Beehler, J.W. and M.S. Mulla, *Effects of organic enrichment on temporal distribution and abundance of culicine egg rafts.* J Am Mosq Control Assoc, 1995. **11**(2 Pt 1): p. 167-71.
38. Gardner, A.M., et al., *Weather variability affects abundance of larval Culex (Diptera: Culicidae) in storm water catch basins in suburban Chicago.* J Med Entomol, 2012. **49**(2): p. 270-6.
39. Marini, G., et al., *The Role of Climatic and Density Dependent Factors in Shaping Mosquito Population Dynamics: The Case of Culex pipiens in Northwestern Italy.* PLoS One, 2016. **11**(4): p. e0154018.
40. Fenchel, T.M. and B.B. Jørgensen, *Detritus Food Chains of Aquatic Ecosystems: The Role of Bacteria*, in *Advances in Microbial Ecology*, M. Alexander, Editor. 1977, Springer US: Boston, MA. p. 1-58.
41. Merritt, R.W., R.H. Dadd, and E.D. Walker, *Feeding behavior, natural food, and nutritional relationships of larval mosquitoes.* Annu Rev Entomol, 1992. **37**: p. 349-76.
42. Giorgio, P.A.d. and J.J. Cole, *BACTERIAL GROWTH EFFICIENCY IN NATURAL AQUATIC SYSTEMS.* Annual Review of Ecology and Systematics, 1998. **29**(1): p. 503-541.
43. Demaio, J., et al., *The midgut bacterial flora of wild Aedes triseriatus, Culex pipiens, and Psorophora columbiae mosquitoes.* Am J Trop Med Hyg, 1996. **54**(2): p. 219-23.

44. Duguma, D., et al., *Bacterial communities associated with culex mosquito larvae and two emergent aquatic plants of bioremediation importance.* PLoS One, 2013. **8**(8): p. e72522.
45. Ponnusamy, L., et al., *Species composition of bacterial communities influences attraction of mosquitoes to experimental plant infusions.* Microb Ecol, 2010. **59**(1): p. 158-73.
46. Ponnusamy, L., et al., *Identification of bacteria and bacteria-associated chemical cues that mediate oviposition site preferences by Aedes aegypti.* Proc Natl Acad Sci U S A, 2008. **105**(27): p. 9262-7.
47. Reiskind, M.H. and M.L. Wilson, *Culex restuans (Diptera: Culicidae) oviposition behavior determined by larval habitat quality and quantity in southeastern Michigan.* J Med Entomol, 2004. **41**(2): p. 179-86.
48. Chaves, L.F., et al., *Combined sewage overflow enhances oviposition of Culex quinquefasciatus (Diptera: Culicidae) in urban areas.* J Med Entomol, 2009. **46**(2): p. 220-6.
49. Lampman, R.L. and R.J. Novak, *Oviposition Preferences of Culex pipiens and Culex restuans for Infusion-Baited Traps.* Journal of the AMerican Mosquito Control Association, 1996. **12**(1): p. 23-32.
50. Chaves, L.F., et al., *Combined sewage overflow accelerates immature development and increases body size in the urban mosquito Culex quinquefasciatus.* Journal of Applied Entomology, 2011. **135**(8): p. 611-620.
51. Yoshioka, M., et al., *Diet and density dependent competition affect larval performance and oviposition site selection in the mosquito species Aedes albopictus (Diptera: Culicidae).* Parasit Vectors, 2012. **5**: p. 225.
52. McCann, S., et al., *Age modifies the effect of body size on fecundity in Culex quinquefasciatus Say (Diptera: Culicidae).* J Vector Ecol, 2009. **34**(2): p. 174-81.
53. Dadd, R.H., *Essential fatty acids for the mosquito Culex pipiens.* J Nutr, 1980. **110**(6): p. 1152-60.
54. Dadd, R.H., *Amino acid requirements of the mosquito Culex pipiens: asparagine essential.* J Insect Physiol, 1978. **24**(1): p. 25-30.
55. Dye, C., *Models for the Population Dynamics of the Yellow Fever Mosquito, Aedes aegypti.* Journal of Animal Ecology, 1984. **53**(1): p. 247-268.
56. Juliano, S.A., *Species Introduction and Replacement among Mosquitoes: Interspecific Resource Competition or Apparent Competition?* Ecology, 1998. **79**(1): p. 255-268.
57. Gillooly, J.F., et al., *Effects of size and temperature on metabolic rate.* Science, 2001. **293**(5538): p. 2248-51.
58. Campbell, A. and R.N. Sinha, *Bioenergetics of granivorous beetles, Cryptolestes ferrugineus and Rhyzopertha dominica (Coleoptera: Cucujidae and Bostrichidae).* Canadian Journal of Zoology, 1978. **56**(4): p. 624-633.
59. Reiskind, M.H., E.T. Walton, and M.L. Wilson, *Nutrient-dependent reduced growth and survival of larval Culex restuans (Diptera: Culicidae): laboratory and field experiments in Michigan.* J Med Entomol, 2004. **41**(4): p. 650-6.
60. Farrar, R.R., J.D. Barbour, and G.G. Kennedy, *Quantifying food consumption and growth in insects.* Annals of the Entomological Society of America, 1989. **82**(5): p. 593-598.
61. Agnew, P., C. Haussy, and Y. Michalakis, *Effects of Density and Larval Competition on Selected Life History Traits of Culex pipiens quinquefasciatus (Diptera: Culicidae).* Journal of Medical Entomology, 2000. **37**(5): p. 732-735.
62. Roberts, D., *Overcrowding of Culex sitiens (Diptera: Culicidae) larvae: population regulation by chemical factors or mechanical interference.* J Med Entomol, 1998. **35**(5): p. 665-9.
63. Wynn, G. and C.J. Paradise, *Effects of microcosm scaling and food resources on growth and survival of larval Culex pipiens.* BMC Ecology, 2001. **1**: p. 3-3.
64. Kaplan, E.L. and P. Meier, *Nonparametric Estimation from Incomplete Observations.* Journal of the American Statistical Association, 1958. **53**(282): p. 457-481.

65. Crouse, D.T., L.B. Crowder, and H. Caswell, *A Stage-Based Population-Model for Loggerhead Sea-Turtles and Implications for Conservation.* Ecology, 1987. **68**(5): p. 1412-1423.
66. Lefkovitch, L.P., *The Study of Population Growth in Organisms Grouped by Stages.* Biometrics, 1965. **21**(1): p. 1-18.
67. Jarry, M., M. Khaladi, and J.P. Gouteux, *A matrix model for studying tsetse fly populations.* Entomologia Experimentalis et Applicata, 1996. **78**(1): p. 51-60.
68. Ciota, A.T., et al., *The Effect of Temperatue on Life History Traits of Culex Mosquitoes.* Journal of Medical Entomology, 2014. **51**(1): p. 55-62.
69. Dadd, R.H. and J.E. Kleinjan, *Dietary nucleotide requirements of the mosquito, Culex pipiens.* J Insect Physiol, 1977. **23**(3): p. 333-41.
70. Anderson, J.F., et al., *Control of mosquitoes in catch basins in Connecticut with Bacillus thuringiensis israelensis, Bacillus sphaericus, [corrected] and spinosad.* J Am Mosq Control Assoc, 2011. **27**(1): p. 45-55.
71. Cailly, P., et al., *A climate-driven abundance model to assess mosquito control strategies.* Ecological Modelling, 2012. **227**: p. 7-17.
72. Knepper, R.G., et al., *Evaluation of methoprene (Altosid XR) sustained-release briquets for control of culex mosquitoes in urban catch basins.* J Am Mosq Control Assoc, 1992. **8**(3): p. 228-30.
73. McCarry, M.J., *Efficacy and persistence of Altosid pellets against Culex species in catch basins in Michigan.* J Am Mosq Control Assoc, 1996. **12**(1): p. 144-6.
74. Vasquez, M.I., et al., *Susceptibility of Culex pipiens (Diptera: Culicidae) field populations in Cyprus to conventional organic insecticides, Bacillus thuringiensis subsp. israelensis, and methoprene.* J Med Entomol, 2009. **46**(4): p. 881-7.
75. Zhang, X., F. Meng, and Q. LIU, *Study on the efficacy of spinosad Natular G30 against Culex pipiens quinquefasciatus in two types of breeding habitats in Hainan, China.* Chinese Journal of Vector Biology and Control, 2014. **25**(2): p. 105-108.
76. Saxena, V., B.G. Bolling, and T. Wang, *West Nile Virus.* Clinical Laboratory Medicine, 2017.

Tables

Table 1. Various larvicides used in urban catch basins and their measured efficacy in field or lab environments [21, 23-26, 70, 72-75].

Larvicide	Observation Type	Activity	Efficacy Period (Days)	Reference
Novaluron	In-Lab	90% Emergence Inhibition (2.359 ± 1.322 ppb)	After day 5	*Su et. al., 2014*
	Field	Reduced Density and Emergence Rate	35	*Su et. al., 2014*
BTI	In-Lab	95% Mortality Rate	N/A	*Vasquez et. al.,2009*
	Field	>90% reduction in larval densities	31	*Cetin et. al., 2015*
	Field	Reduced Larval Densities	14	*Anderson et. al., 2011*
Methoprene (Altosid)	In-Lab	99% Emergence Inhbition	N/A	*Knepper et. al., 1992*
	In-Lab	95% Mortality Rate	N/A	*Vasquez et. al.,2009*
	Field	70% Emergence Inhibition	105	*Knepper et. al., 1992*
	Field	>90% Emergence Inhibtion	58	*McCarry, 1996*
Spinosad (Natular)	Field	Reduced Density and Emergence Rate	63	*Harbison et. al., 2014*
	Field	Reduced Density and Emergence Rate (<20 mg/m^2)	12	*Zhang et. al., 2014*
	Field	Reduced Density and Emergence Rate (>20mg/m^2)	>30	*Zhang et. al., 2014*
	Field	Reduced Larval Densities	35	*Anderson et. al., 2011*
	Field	99% Mortality Rate	7-105	*Harbison et. al., 2016*
	Field	Reduced Density across 73% of samples	N/A	*Harbison et. al. 2014*

Table 2. Each treatment, consisting of a starting nutrient availability and daily addition, was replicated across five mosquito breeders.

Treatment ID	Starting Nutrient Concentration	Starting Nutrient Availability	Stock added Daily
High (HI)	0.3 mg/mL	120 mg	9 mg
Mid High (MH)	0.15 mg/mL	60 mg	4.5 mg
Mid Low (ML)	0.075 mg/mL	30 mg	2.25 mg
Low (LO)	0.0375 mg/mL	15 mg	1.125 mg

Table 3. List of metrics used in the calculation of model parameters

Parameter	Description
$\mathbf{N_t}$	Population at time t
$\boldsymbol{\omega(t)}$	Resources available over time within an experimental treatment
$\boldsymbol{\omega_t}$	Resources available within an environment at time t
K	Number of individuals a habitat can support (carrying capacity)
$\mathbf{C_\omega(t)}$	Experimentally determined consumption rate function for resource treatment group ω
$\mathbf{C_j}$	Consumption rate that determines metabolic age of cohort j
$\boldsymbol{\Omega_j}$	Coefficient of competition showing exploitative effects of all cohorts present in an environment on cohort j
d	The metabolic cohort that I instar larvae join upon hatching
$\mathbf{d_f}$	The highest metabolic cohort that newly hatched larvae can join
$\boldsymbol{\mu_\omega}$	Mortality curve of a given resource treatment group ω
$\mathbf{S_\omega(t)}$	Survivorship over time within resource treatment group ω
$\mathbf{S_{j.t}}$	The survivorship of cohort j at time t
Z	The final metabolic age cohort in the model with the largest consumption rate

Table 4. Survivorship and metamorphosis rates in larval competition experiments.

Nutrient Treatment	**Survivorship ± 95%CI**	**Stage Change Rate (Days) ± 95%CI**
High (t_0 = 3 mg/larva)	-	-
Larval Pupation	99.0 ± 1.0	12.2 ± 3.43
Pupal Emergence	98.5 ± 1.0	-
Total Emergence	97.5 ± 1.6	15.2 ± 3.3
Mid-High (t_0 = 1.5 mg/larva)	-	-
Larval Pupation	94.5 ± 3.9	15.4 ± 7.3
Pupal Emergence	94.5 ± 2.0	-
Total Emergence	95.0 ± 4.3	18.42 ± 7.4
Mid-Low (t_0 = 0.75 mg/larva)	-	-
Larval Pupation	48.5 ± 7.1	23.8 ± 13.2
Pupal Emergence	99.0 ± 1.0	-
Total Emergence	51.5 ± 7.4	26.6 ± 12.6
Low (t_0 = 0.375 mg/larva)	-	-
Larval Pupation	23.5 ± 11.6	31.7 ± 14.0
Pupal Emergence	93.0 ± 5.0	-
Total Emergence	24.0 ±5.7	33.9 ± 12.3

Table 5. Generalized Linear Models of mortality curves in low nutrient environments. Listed are the slopes, intercepts and significance of these prediction functions.

Nutrient Treatment	**Slope ± 95%CI**	**Intercept ± 95%CI**	**P-Value**
Mid-High (t_0 = 1.5 mg/larva)	0.1 ± 0.04	2.0 ±0.10	p << 0.001
Mid-Low (t_0 = 0.75 mg/larva)	1.1 ± 0.06	5.7 ± 2.4	p << 0.001
Low (t_0 = 0.375 mg/larva)	1.5 ± 0.12	14.9 ± 3.5	p << 0.001

Table 6. The Model N* (above) utilizes a stage-based matrix projection with daily transitions for each parameter. Model A (below) uses these same parameters but instead substitutes an environmentally determined larval survivorship matrix that enumerates each metabolic age. Below are the values used for the transition matrix of the projection cycle. Blue denotes survivorship while red denotes stage change. Fecundity of gravid females is shown in beige. Placement of newly hatched larval cohorts within the model projection cycle occurred within the function d(ω), the calculated metabolic age upon hatching given the nutrients present in the environment within the range 1 to d_f (39).

	Eggs	Larvae	Pupae	Adults	Gravid Adults
Eggs	0	0	0	0	260
Larvae	0.93	0.64	0	0	0
Pupae	0	0.02	0.5	0	0
Adults	0	0	0.5	0.81	0.45
Gravid Adults	0	0	0	0.09	0

	Eggs	L1	L2	L3	L4-38	L39	L40	L41	L42	L.Z = 43	Pupae	Adults	Gravid Adults
Eggs	0	0	0	0	0	0	0	0	0	0	0	0	260
L1	d(μ) = 0.93	0	0	0	0	0	0	0	0	0	0	0	0
L2		S(μ, CR_1)	0	0	0	0	0	0	0	0	0	0	0
L3		0	S(μ, CR_2)	0	0	0	0	0	0	0	0	0	0
L4-38		0	0	S(μ, CR_3)	0	0	0	0	0	0	0	0	0
L39		0	0	0	S(μ, CR_{4-38})	0	0	0	0	0	0	0	0
L40	0	0	0	0	0	S(μ, CR_{39})	0	0	0	0	0	0	0
L41	0	0	0	0	0	0	S(μ, CR_{40})	0	0	0	0	0	0
L42	0	0	0	0	0	0	0	S(μ, CR_{41})	0	0	0	0	0
L.Z = 43	0	0	0	0	0	0	0	0	S(μ, CR_{42})	0	0	0	0
Pupae	0	0	0	0	0	0	0	0	0	0.66	0.5	0	0
Adults	0	0	0	0	0	0	0	0	0	0	0.5	0.81	0.45
Gravid Adults	0	0	0	0	0	0	0	0	0	0	0	0.09	0

Table 7. Relative abundance of adult species in the Baker woods study area. Values shown are aggregate female collections over the course of 6 weeks in three light trap locations.

Genus	**species**	**Total**	**Females/Trap/night**	**SE**	**Proportion**
Culex	*quinquefasciatus*	43	2.39	0.99	0.28
	spp.	34	1.89	0.72	0.22
	restuans	7	0.39	0.14	0.05
	All	84	4.67	1.67	0.54
Aedes	*albopictus*	57	3.17	1	0.37
	vexans	5	0.61	0.18	0.07
Ochlerotatus	*triseriatus*	11	0.28	0.18	0.03
	Total	156	8.67	2.61	

Table 8. Sensitivity analysis of Model A based on consumption rate. Total Proliferation, efficiency, and time to extinction varied with altered consumption parameters. Apart from calculation of carrying capacity (K) and time to extinction, numbers in gray are absolute while white are proportional responses to Model A by the respective changes in consumption.

	Model B	**Model A**	**Model C**
Base Consumption	0.53	0.4	0.26
	1.33	1	0.66
Eggs Oviposited (100 days)	193000	220000	377000
	0.88	1	1.71
Adults Emerged (100 days)	13000	14000	21000
	0.9	1	1.53
Nutrients consumed (kg; 100 days)	5.2	5.9	10.4
	0.88	1	1.75
Nutrients Consumed / Emergence (mg/adult)	410	420	480
	0.97	1	1.14
Eggs Oviposited / Emergence (egg/adult)	15	16	18
	0.94	1	1.14
K Estimate (t = 0)	23000	25000	57000
	0.9	1	2.25
K Estimate (t = 100)	21000	24000	52000
	0.88	1	2.17
Time to Extinction (Days)	1600	2500	1300
	0.64	1	0.52

Figures

Figure 1. The West Nile Virus Transmission Cycle [76]

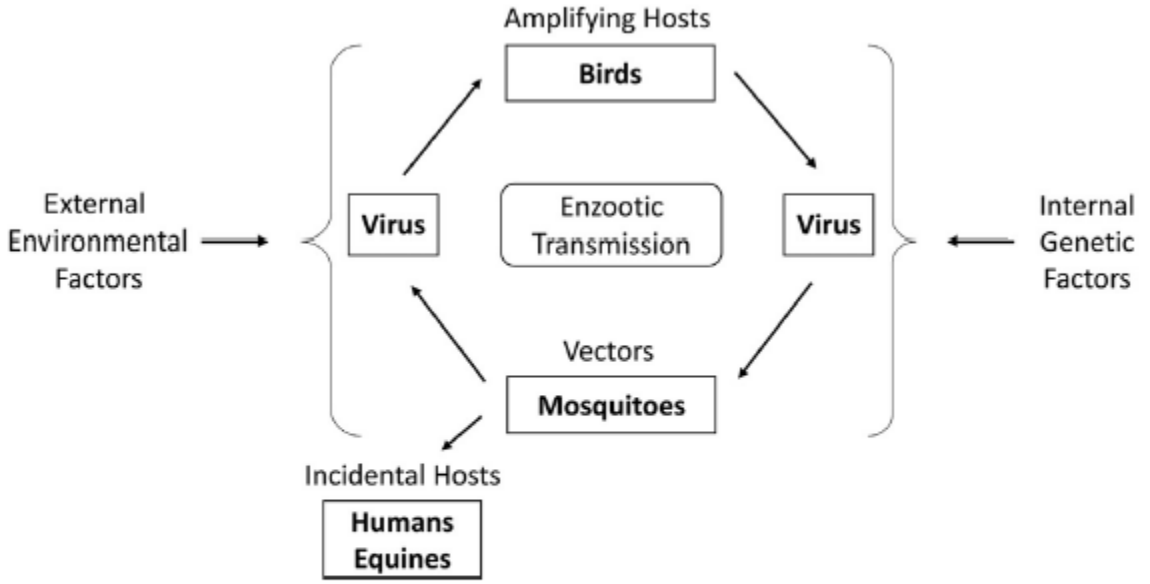

Fig. 1. West Nile virus transmission cycle. The virus is maintained in nature by an enzootic transmission cycle between mosquitoes and avian hosts. Humans and horses are considered incidental or "dead-end" hosts, as they do not generate sufficient viremia to support ongoing transmission. Numerous external environmental factors and internal genetic factors can affect the transmission cycle.

Figure 2. A diagram of the catch basin habitat found in urban environments [31]. The basin collects standing water and debris from surrounding surface areas.

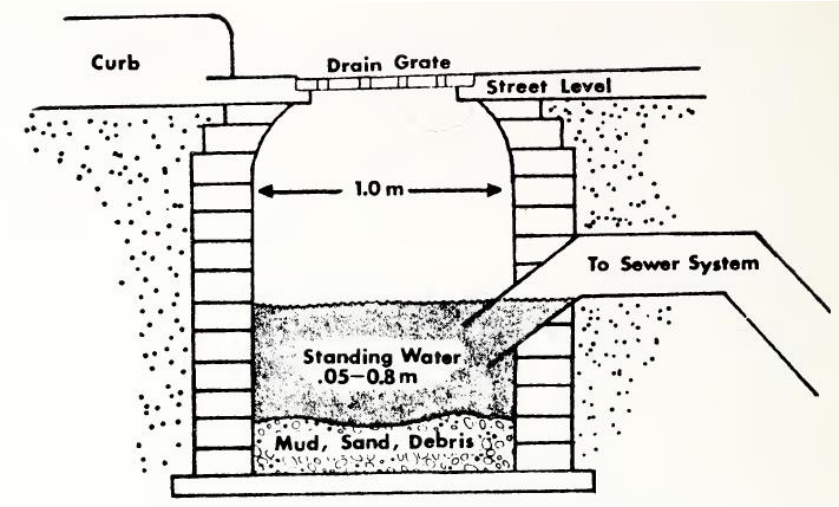

Figure 3. Methods Flow Chart. Arrows point in the direction of which data or parameter informs the next while darker arrows denote higher gravity of information.

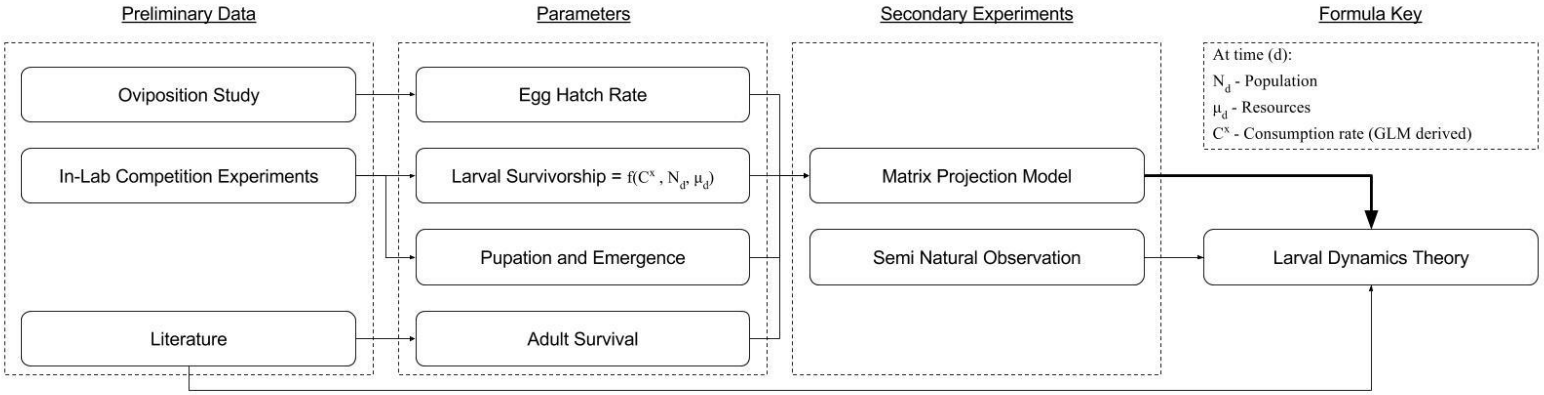

Figure 4. BioQuip Mosquito Breeders (A) were used to rear larvae (B) and pupae (C) in the lower compartment and house adults (D) in the upper compartment. Both C and D show molts of IV instar larvae and pupae, respectively. D was taken during the 25°C pilot study.

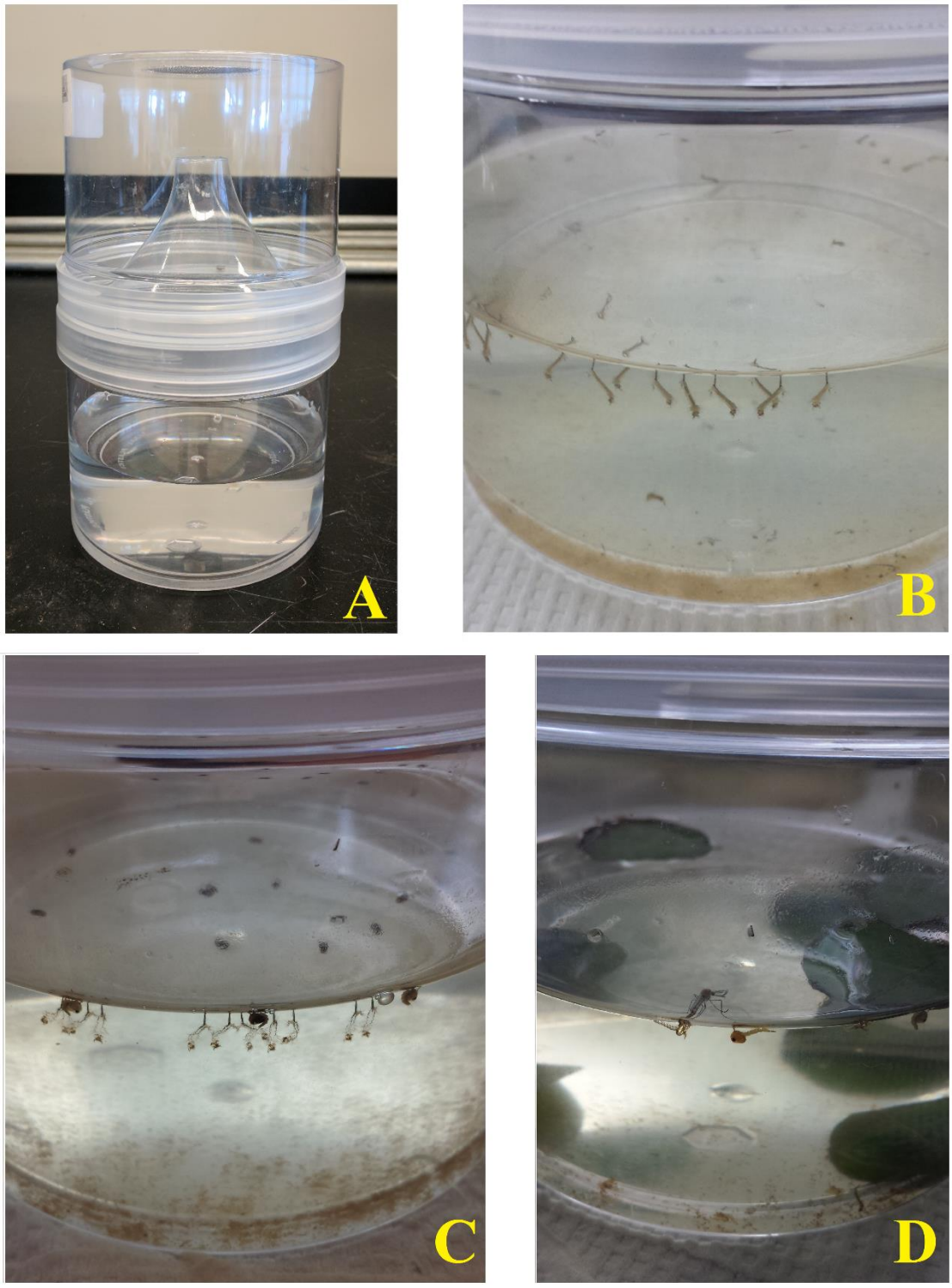

Figure 5. Container used as a mesocosm during the semi-natural observation study.

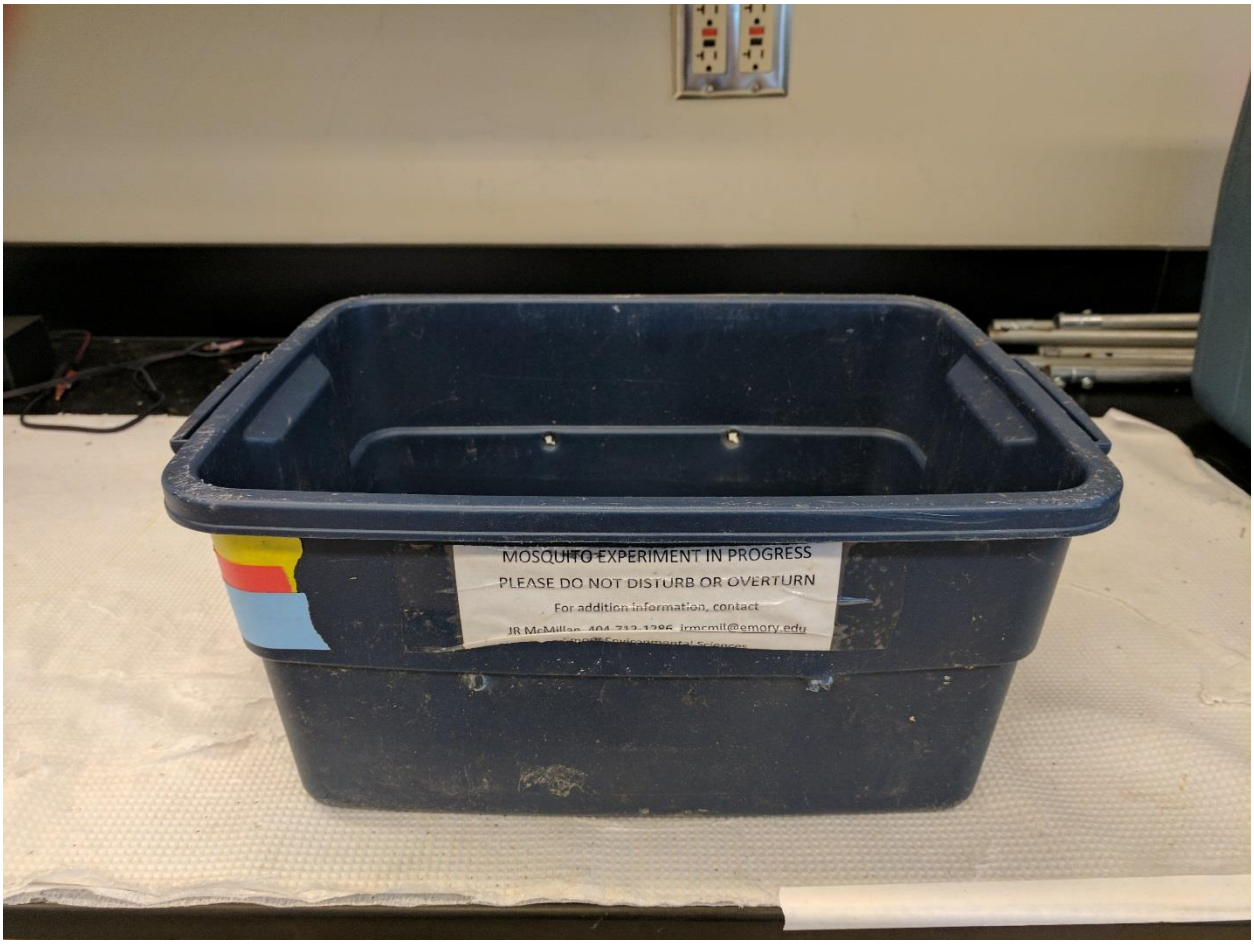

Figure 6. Diagram of a light trap courtesy of Fairfax County Health Department.

Figure 7. The matrix projection cycle, illustrating the four life history stages of *Cx. quinquefasciatus* (egg, larva, pupa, adult). The larval submatrix is shown as a day by day event that is calculated in terms of survivorship by the amount of resources available in the environment at a given time.

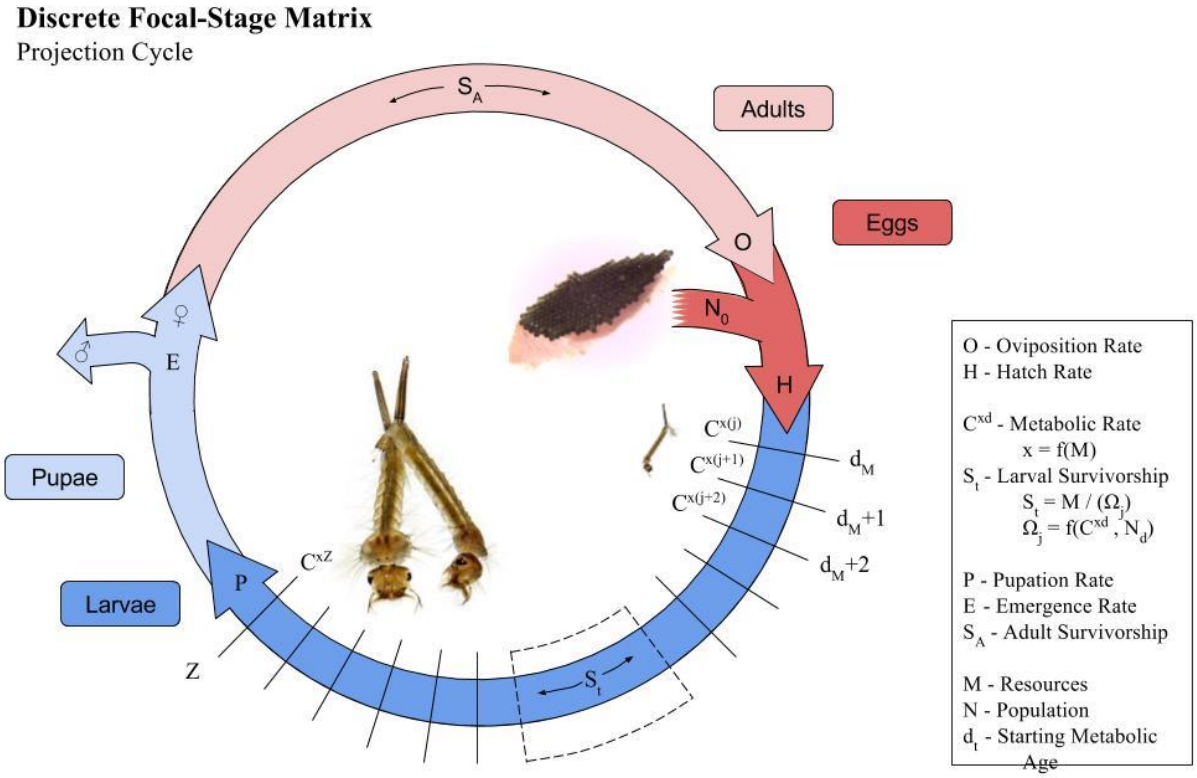

Figure 8. The structural difference between Model N* (stage-based) and Model A (focal-stage). Blue zones indicate same-stage survivorship while red zones indicate stage change. Each zone is labeled in binary as a starting stage (first letter abbreviation; e.g. E = Eggs) and end stage (second letter). Fecundity is labeled separately in beige.

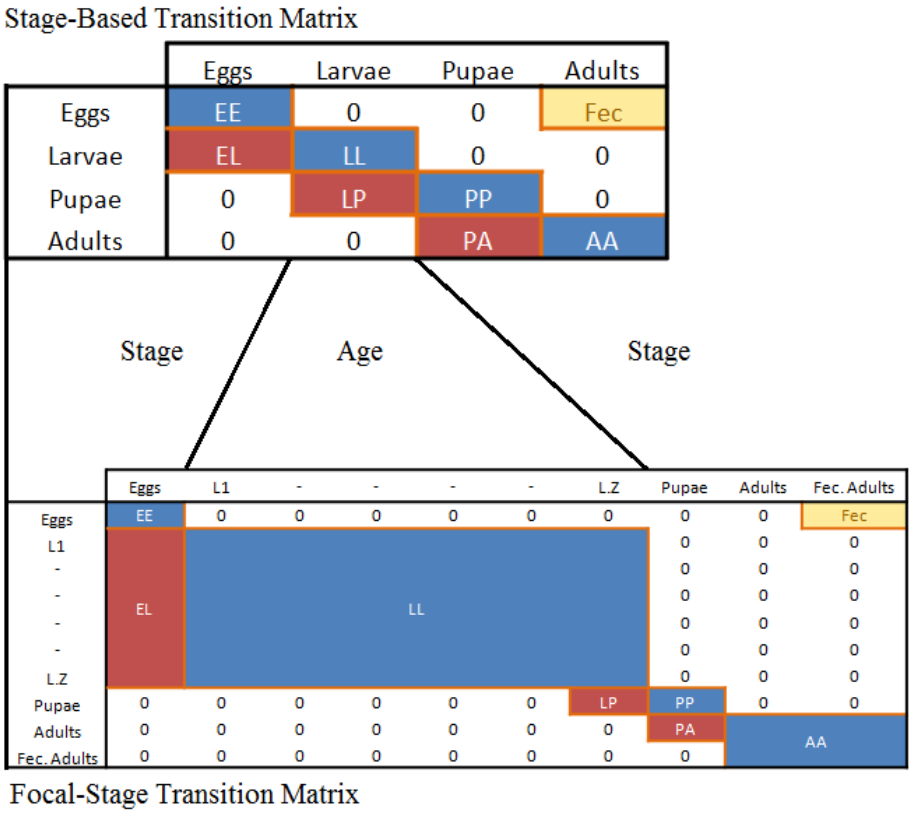

Figure 9. Absolute (top) and relative (bottom) rates of stage change in larval competition experiments with high to low nutrient availability per capita. Absolute time to emergence shows significant groupings by result of Tukey HSD. Emergence of pupae remains relatively constant while range and length of time to pupation by larvae increases with lower nutrient treatments.

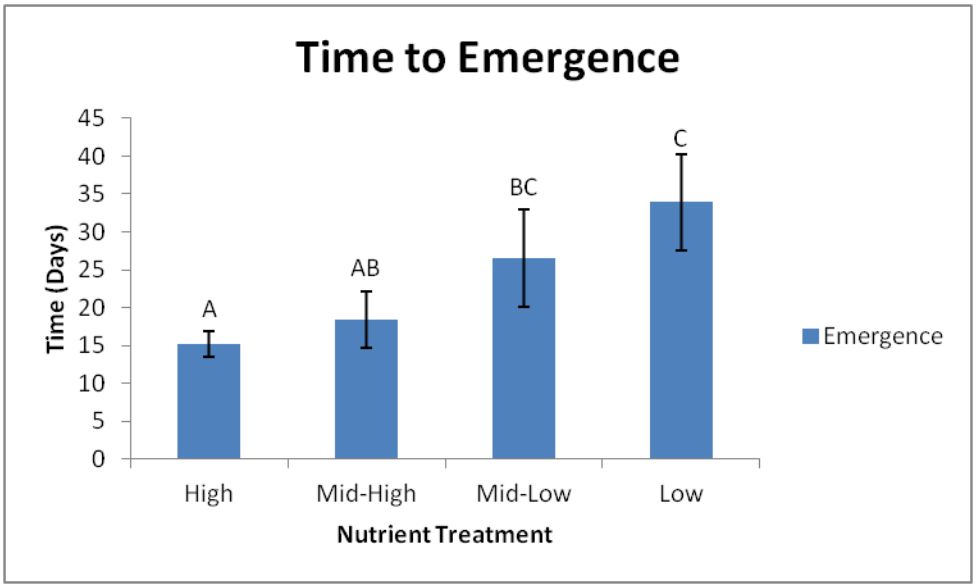

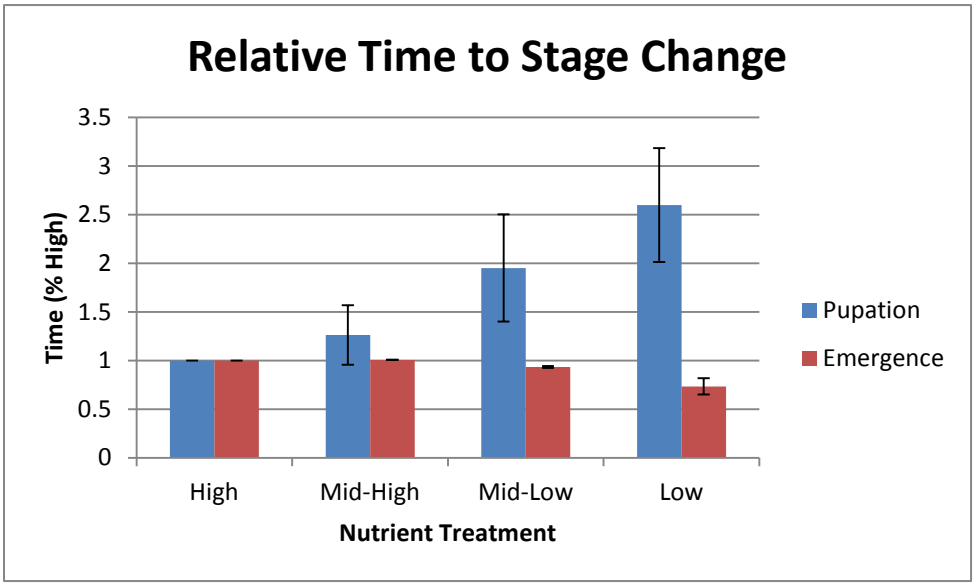

Figure 10. Survivorship to the next stage (larvae to pupae in blue, pupae to adults in red) shows variable response to competition by stage. Bars are labeled by significantly similar groupings by Tukey HSD analysis.

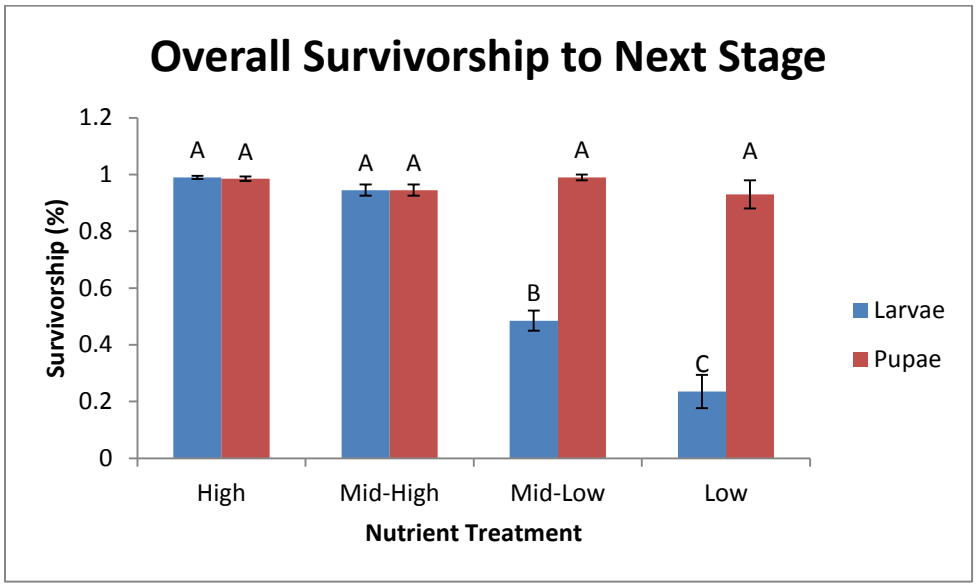

Figure 11. Mortality rates of nutrient treatments within the larval competition experiment. Points illustrate observed values while the linear trends show GLM predicted curves.

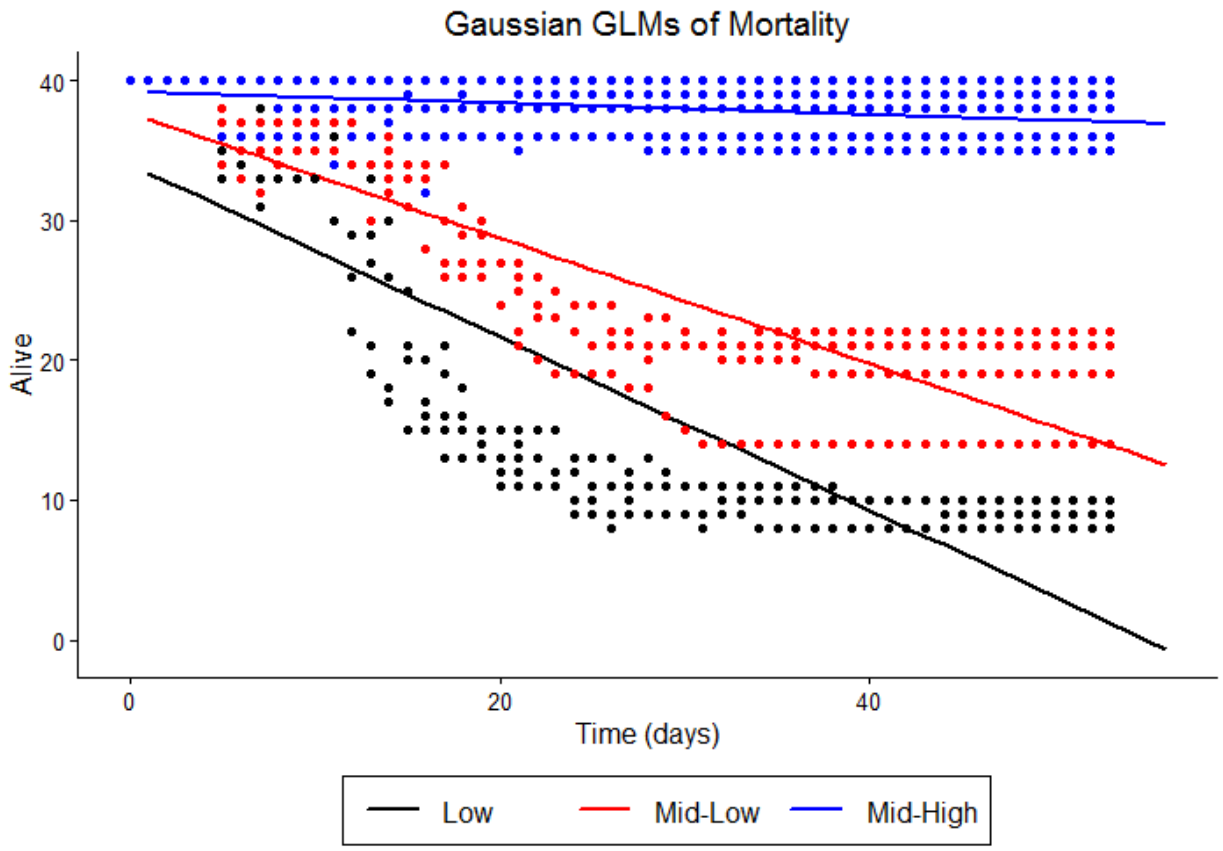

Figure 12. The predicted consumption rates of the three lower nutrient treatments with competition responses

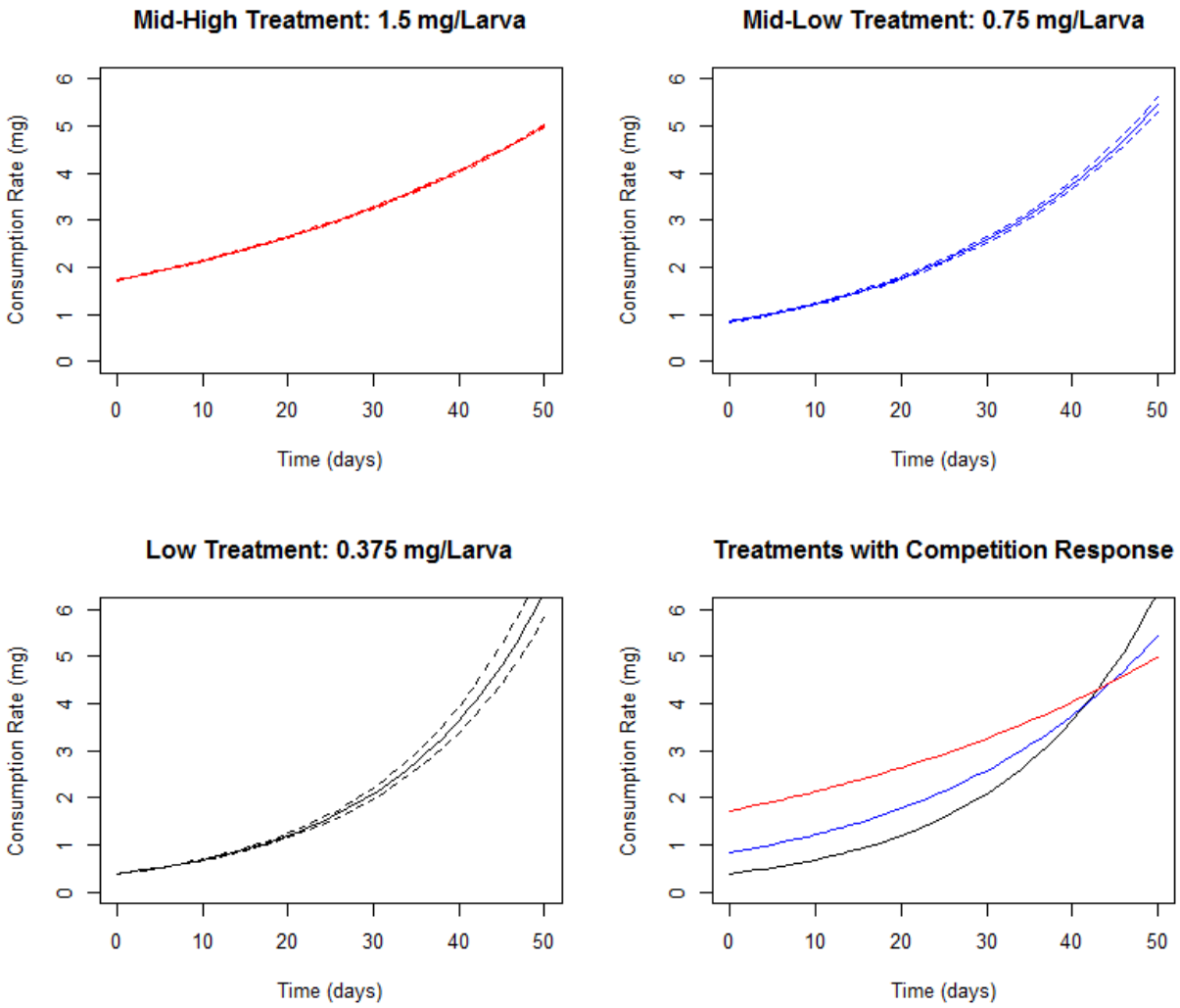

Figure 13. Predicted cumulative consumption across treatments shows mass accumulation synchrony in observed values despite variable temporal distribution. Vertical lines show the day at which pupation occurred for each treatment in corresponding color. The horizontal intercept shows the association of time to pupation with predicted lifetime consumption: (± 95%CI) 32.05 ± 0.07 mg per larvae.

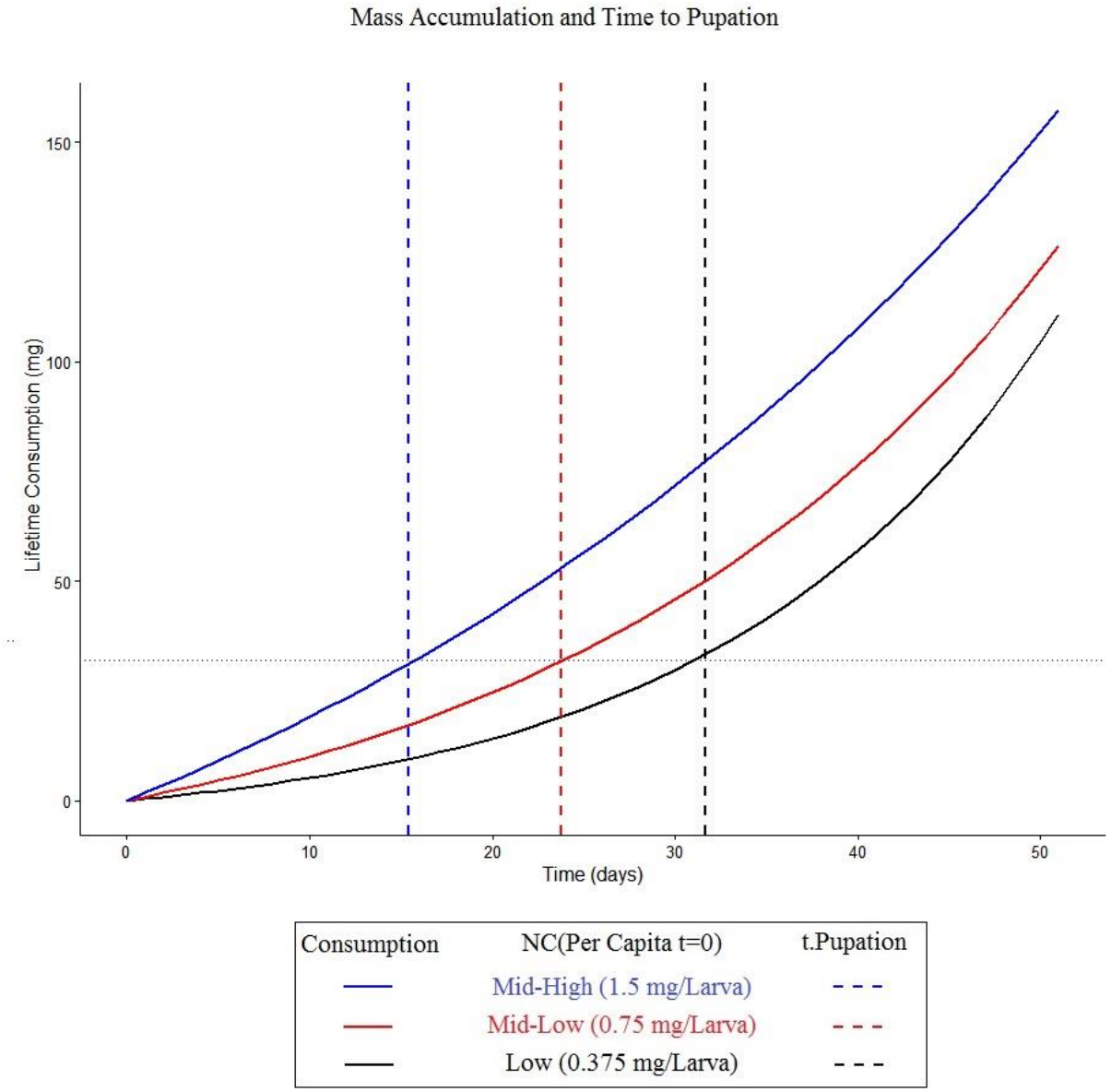

Figure 14. A sample model run with a rain event at day 10, a starting population of 200 non-parous adults.

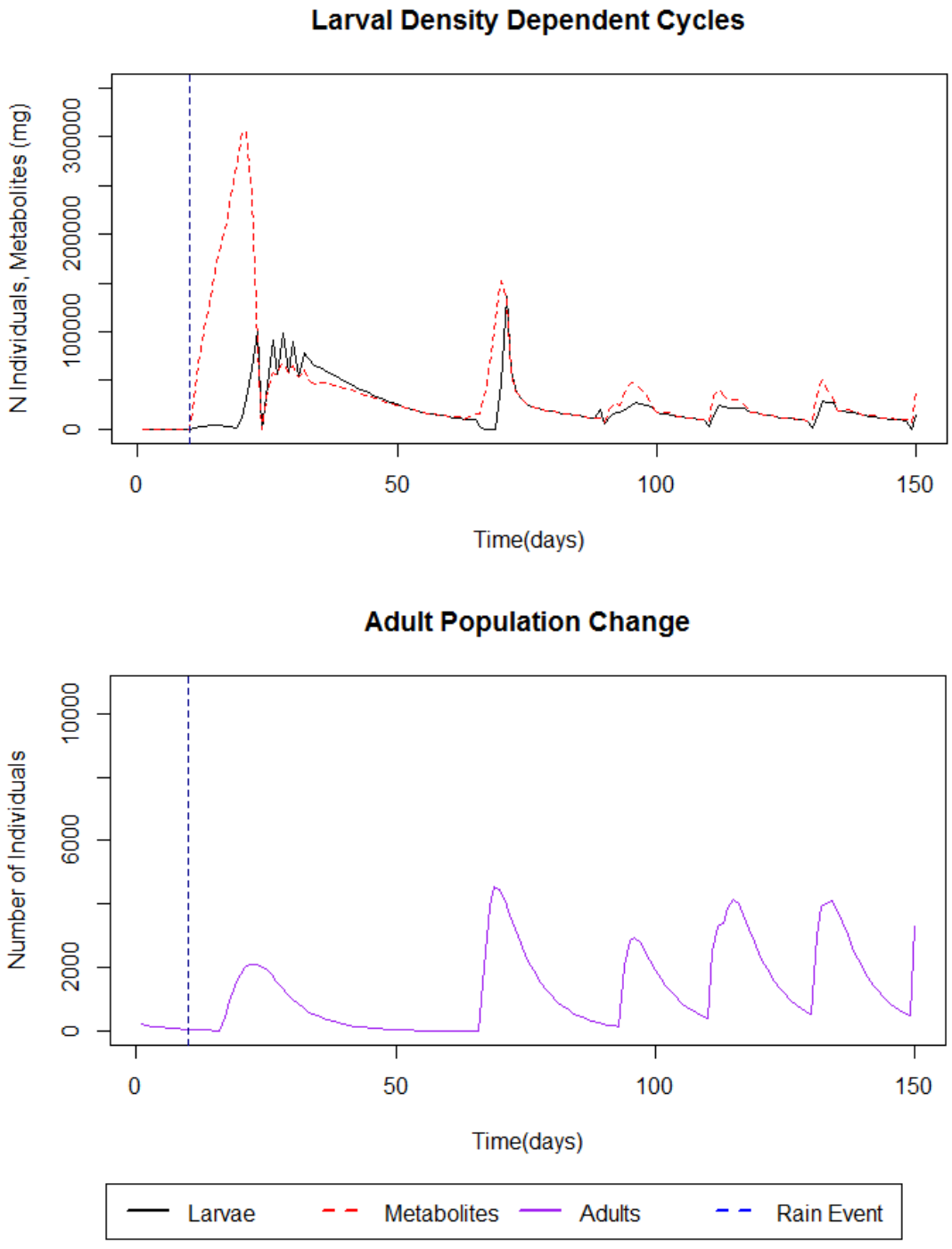

Figure 15. The metabolic age distribution of a population before and after a rain event simulated at day 135. Pre-Rain takes the distribution over t = 100 through 134 while Post-Rain takes the distribution over t = 136 through 175. Post-Period, No Rain shows t = 136 through 175 without a rain event. Red points are the means of the distributions.

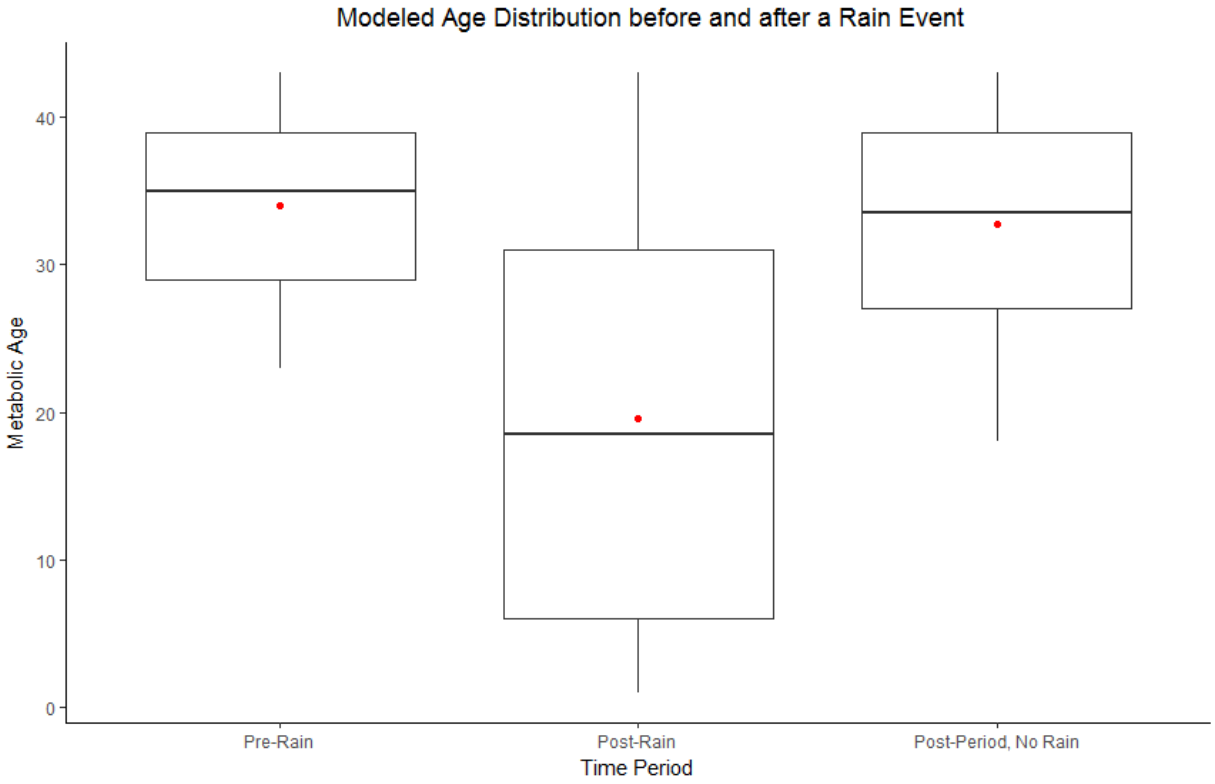

Figure 16. LOESS Regression curves visually show the trends of adult proliferation in Model N* and Model A across variable rainfall periodicity. Baseline proportion is a comparison of a paired event simulation with a single event simulation on the same first day (t = 2). The vertical line in Model A (delay = 19) is the peak of proliferation enhancement, upregulating by ~50%.

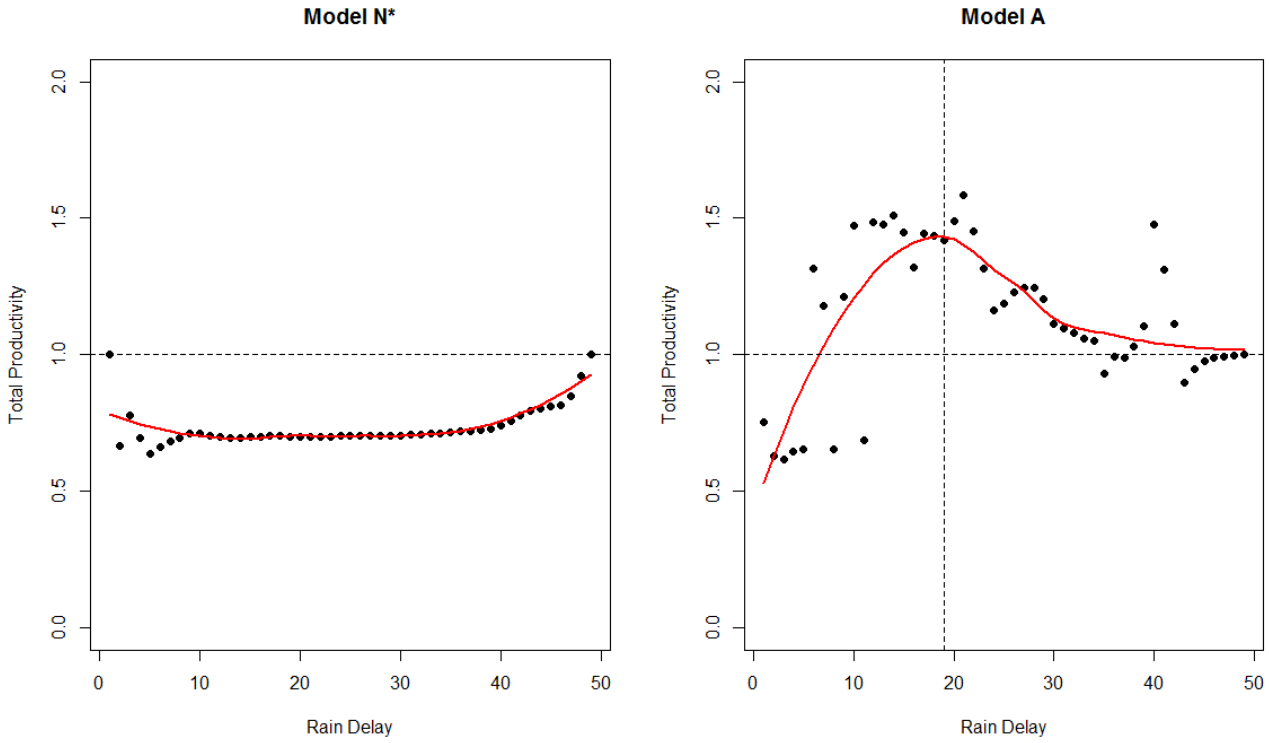

Figure 17. Boxplots of Model A rain delay simulations where each plot shows the range of proliferation rates for that week relative to baseline proliferation from a single rain event.

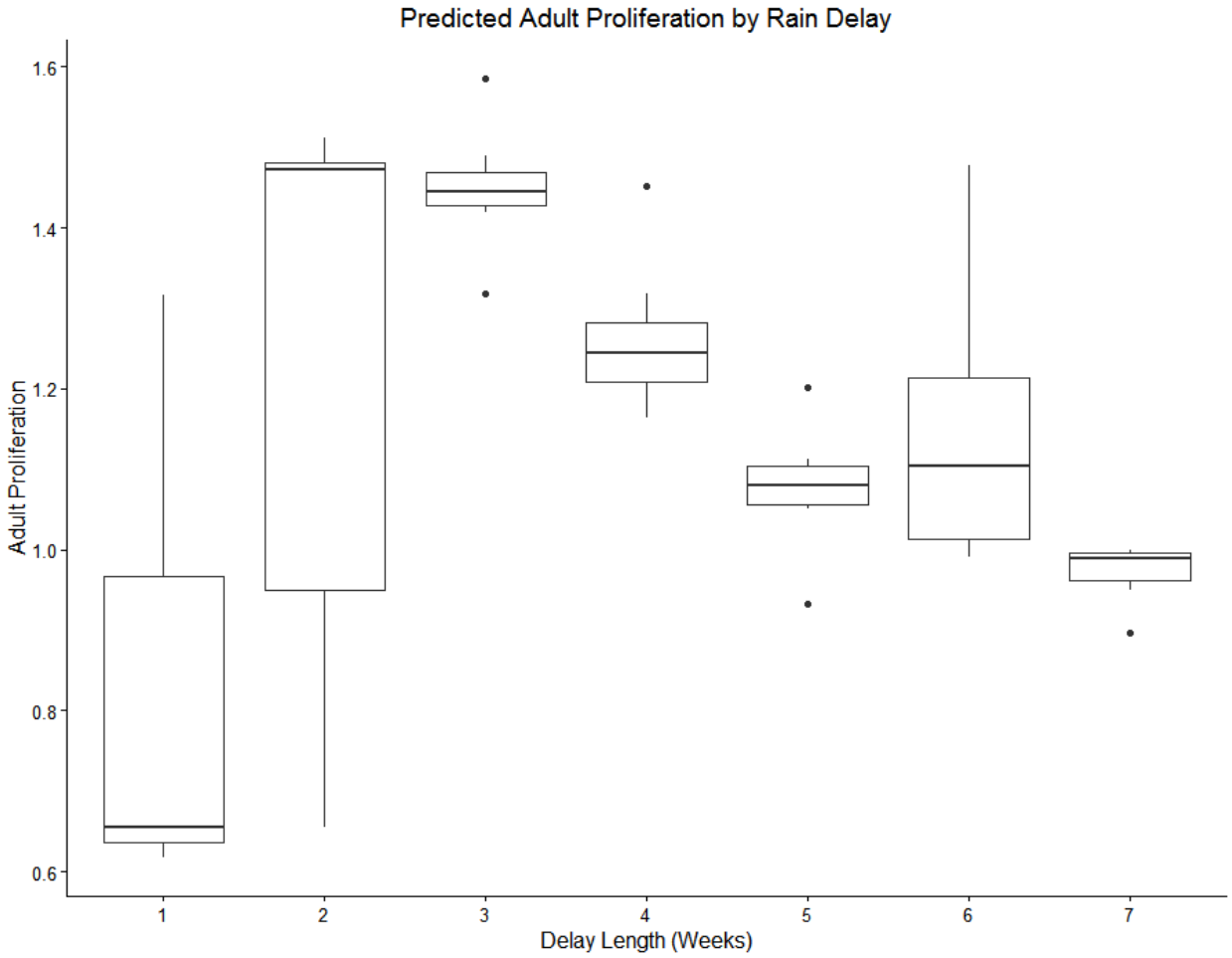

Figure 18. Sensitivity analysis of the Model A simulation shown in Figure 10 through increased and decreased consumption rates.

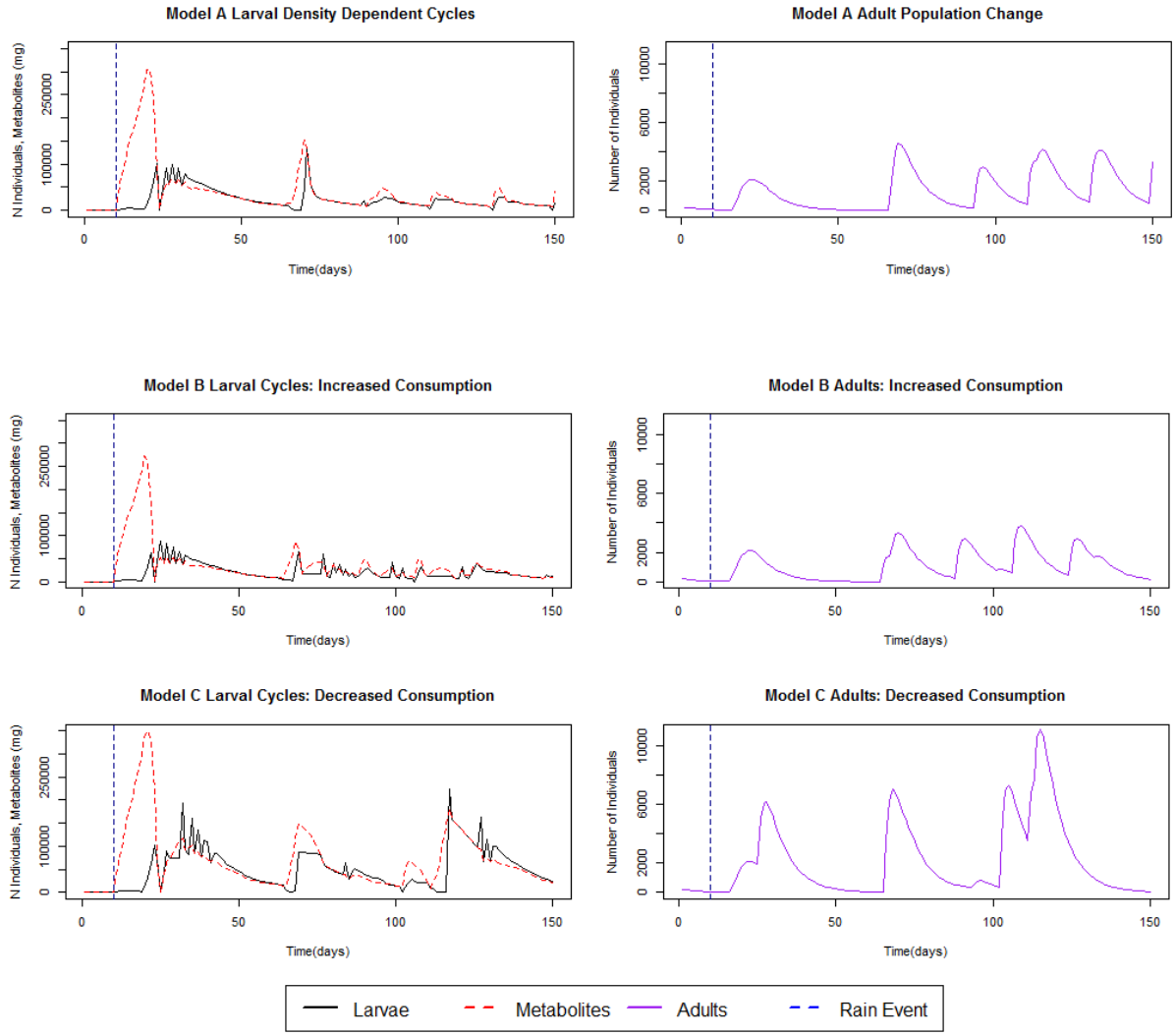

Figure 19. LOESS Regression curves visually show the trends of adult proliferation in Model B and Model C across variable rainfall periodicity. Baseline proportion is a comparison of a paired event simulation with a single event simulation on the same first day (t = 2). The solid blue lines are the base and peak values of Model A.

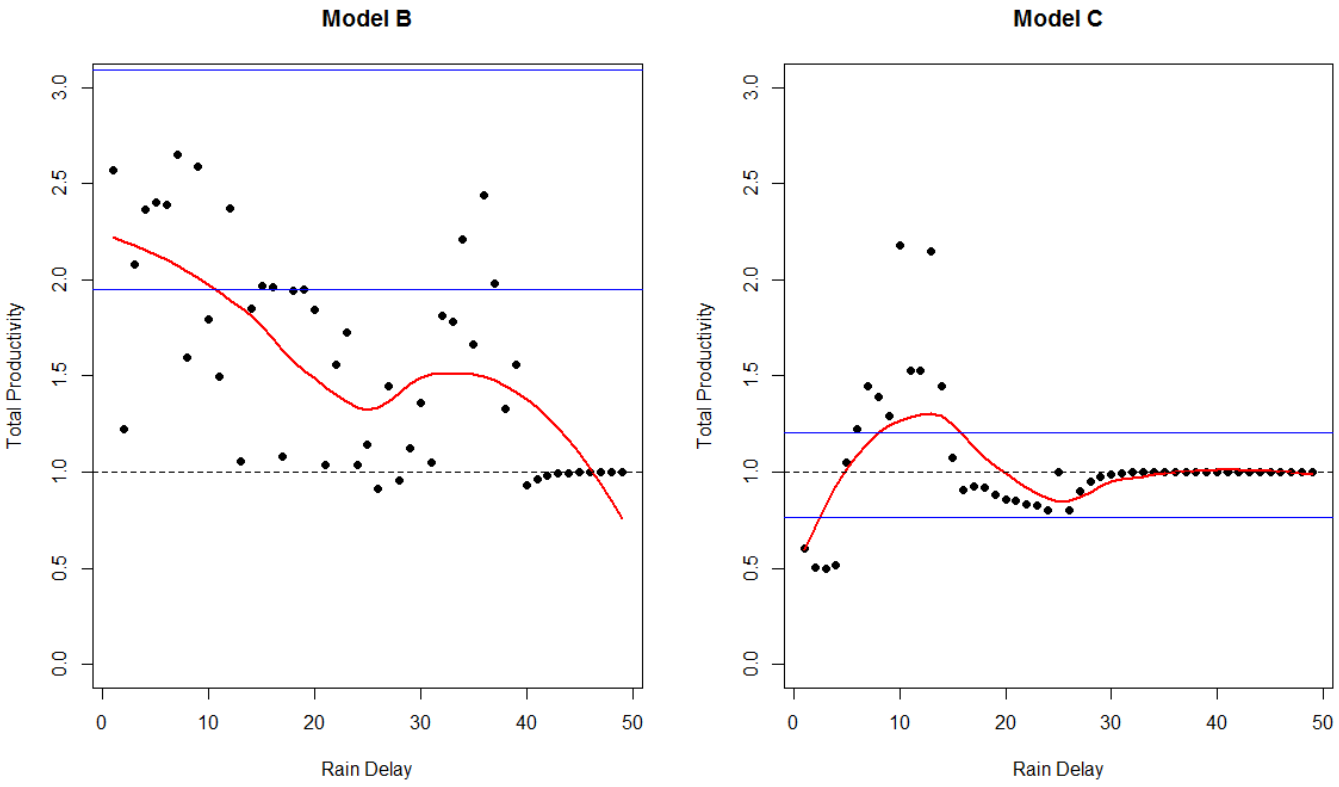

Figure 20. Semi-natural observed larval counts (points) alongside LOESS regressions of each mesocosm (red). The division of each treatment type shows starting nutrient concentration and the LOESS curves for each of the three replicates within that treatment group. There is significant clustering of larvae around high nutrient mesocosms due to preferential oviposition

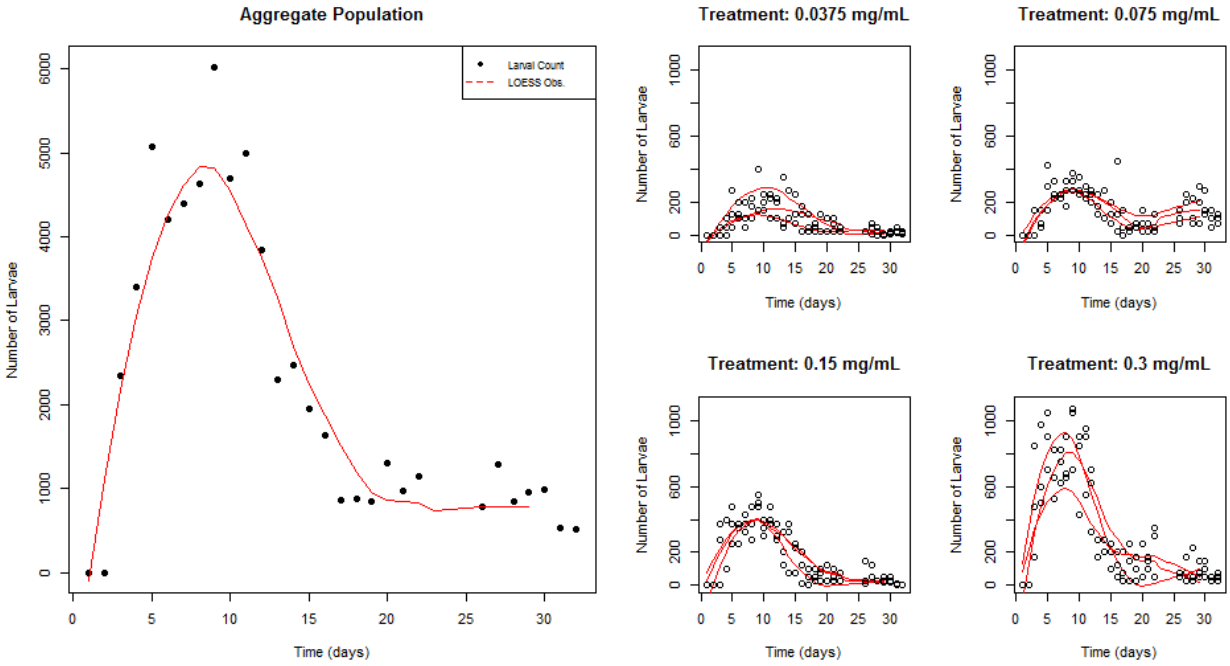

Figure 21. A) The shapes of a simulated proliferation curve and an observed semi-natural curve for larvae (black LOESS) and pupae (red). In both cases there is early pupation for a small subset of individuals while the rest persist in the low nutrient environment. B) The time to completion for a larval proliferation curve in Model A is half the time of decline in semi-natural mesocosms.

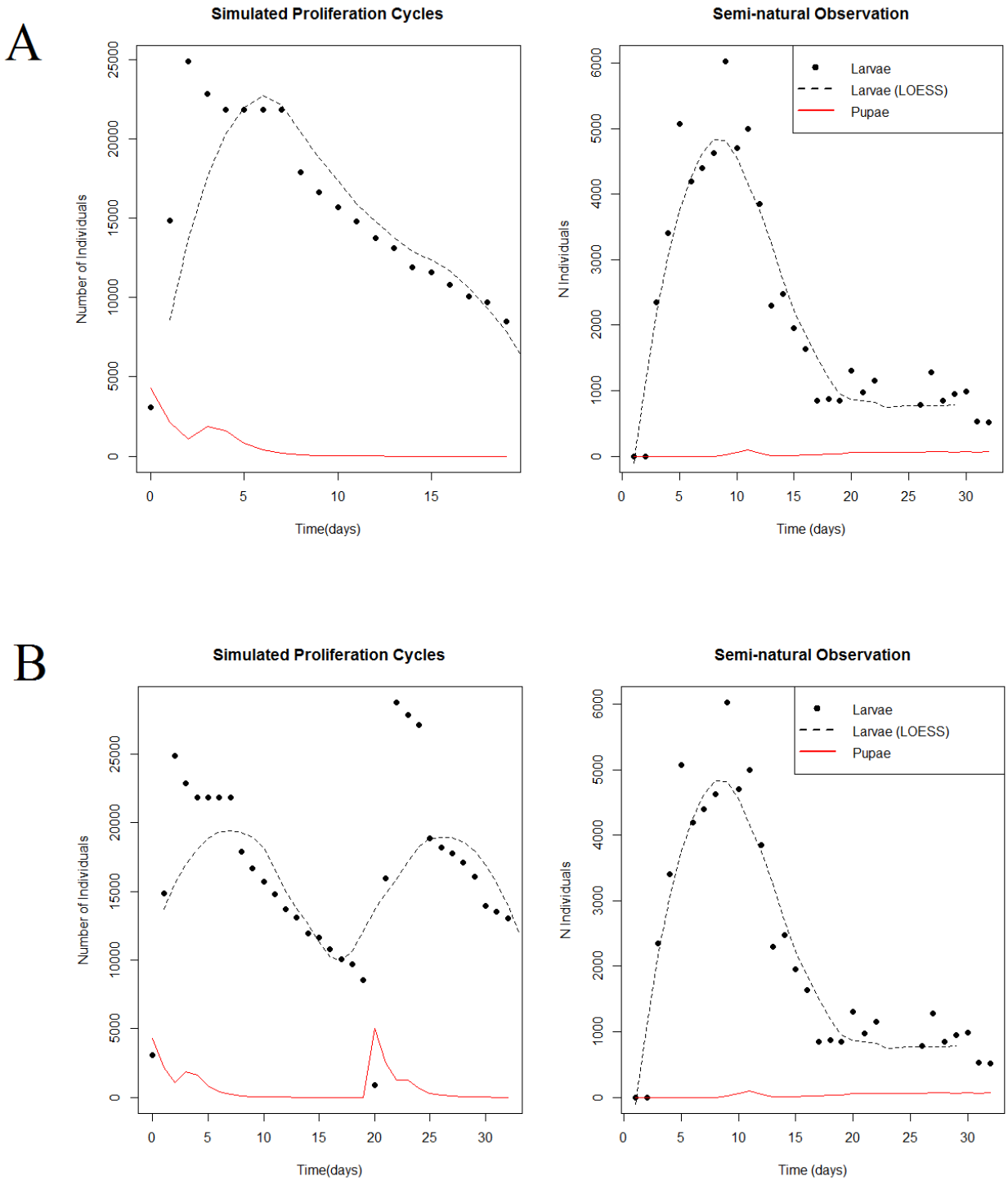

Figure 22. The effect of insecticide treatment on age distribution before and after a rain event. Only IV instar larvae were affected by the larvicidal treatment, simulated in this case for a period of 35 days.

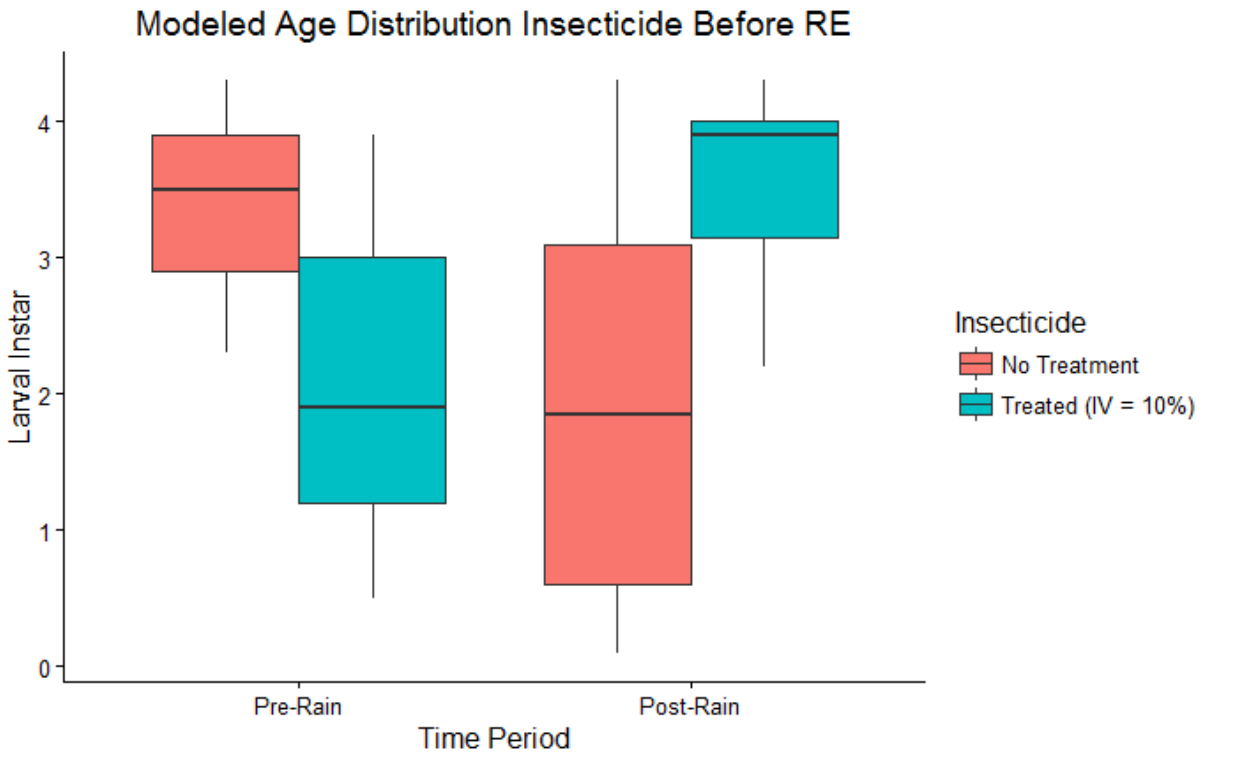

Figure 23. Delayed proliferation and age synchrony may lead to spikes in adult productivity that are more likely to cause the transmission of disease. In the case of rain events supplying nutrients to a vacant immature population (right), proliferation can exceed baseline growth.